SAFETY OF FOUNDATIONS AGAINST LIQUEFACTION

by

KOTARO TANAKA

Master of Engineering, Civil Engineering, Nagoya University, Nagoya, Japan (1988)

Bachelor of Engineering, Civil Engineering, Nagoya University, Nagoya, Japan (1986)

Submitted to the Department of

Civil and Environmental Engineering in Partial Fulfillment of

the Requirements for the

Degree of

MASTER OF SCIENCE

in Civil and Environmental Engineering
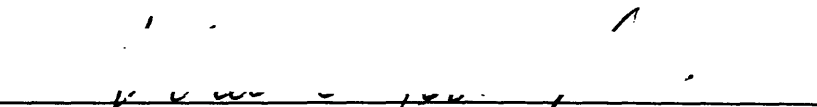
at the

Massachusetts Institute of Technology

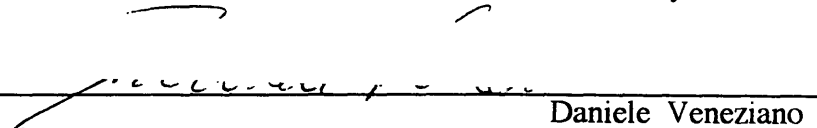February 1995

© 1995 Kotaro Tanaka

All rights reserved

The author hereby grants to MIT permission to reproduce and to distribute publicly paper and electronic copies of this thesis document in whole or in part.

Signature of Author _____
Department of Civil and Environmental Engineering
January 20, 1995

Certified by _____
Daniele Veneziano
Professor
Thesis Supervisor

Accepted by _____
Joseph M. Sussman
Chairman, Departmental Committee on Graduate Students

Barker Eng

MAR 07 1995

SAFETY OF FOUNDATIONS AGAINST LIQUEFACTION

by

KOTARO TANAKA

Submitted to the Department of Civil and Environmental Engineering
on January 20, 1995 in partial fulfillment of the requirements
for the Degree of Master of Science in Civil and Environmental Engineering

ABSTRACT

This study develops a methodology to evaluate the safety of foundations against liquefaction, taking into account (1) the fraction of liquefied area to total area and its variability, (2) the spatial variation of liquefied area, and (3) the vulnerability of the foundation.

The variability in the fraction of liquefied area depends on many unknown parameters. The spatial variation of liquefied area is also complicated and hard to obtain deterministically. Therefore, we describe the spatial pattern of liquefaction/non-liquefaction through a binary (0-1) random field. Two random field models are considered: (1) a spatially continuous model, and (2) a spatially discrete model. Since the vulnerability of foundations to liquefaction varies from foundation to foundation, it is difficult to obtain analytical solutions concerning the safety of foundations. Thus, we rely on numerical simulation. Failure or survival in each simulation is determined by the spatial pattern of liquefied area and the failure criterion of the foundation. By iterating this procedure a number of times, we evaluate the safety of the foundation against liquefaction.

Four one-dimensional cases (two different types of foundations and two different criteria for each foundation) are considered. Generation to two dimensions is also discussed.

Thesis Supervisor :   Dr. Daniele Veneziano

Title :   Professor of Civil and Environmental Engineering

ACKNOWLEDGMENTS

TABLE OF CONTENTS

LIST OF FIGURES

LIST OF FIGURES (CONTINUED)

7

LIST OF TABLE

CHAPTER I. INTRODUCTION

Since the 1969 Niigata earthquake, an event which caused catastrophic failures of buildings and bridges and the consequent loss of lives due to liquefaction, a great deal of effort has been devoted to understanding the mechanism of liquefaction and to evaluating liquefaction susceptibility. Several approaches have been established to deal with common engineering problems. However, since the research completed so far has focused mainly on liquefaction susceptibility at a single point in the ground, we cannot directly predict a failure or survival of laterally extended foundations using the research results. The safety of large foundation systems depends on the two or three-dimensional distribution of liquefied portions in a soil deposit. The engineer's goal is to determine whether a planned structure[1] is safe or not and to evaluate its safety in terms of probability. In this sense, the engineer's demand has not been satisfied completely.

Liquefaction is affected by a number of factors, such as characteristics of the ground (e.g. soil properties, water table), and characteristics of earthquake (e.g. duration of shaking, peak ground acceleration). It is obvious that these factors vary horizontally and with depth. The safety of laterally extended foundations, in general, depends on :

1) the fraction of liquefied area and its variability

2) the spatial variation of liquefied area

3) the vulnerability of foundations

This research examines these factors and proposes a methodology to evaluate the safety of foundations in terms of probability.

The fraction of liquefied area is generally uncertain. Since characteristics of ground and earthquake are also uncertain and few data have been collected in terms of

---

[1] The ground beneath it is subjected to liquefaction.

liquefied area in actual earthquakes, it is hard to specify the fraction of liquefied area and its variability. We cannot but count on engineering judgments at present.

Sounding data at a given site are usually very limited and knowledge concerning the spatial variability of ground and earthquake characteristics is uncertain. In addition, the failure criteria of foundations differ from foundation to foundation. Therefore, we cannot avoid resorting to numerical simulation treating these uncertain factors as random variables.

We need to know the spatial distribution of liquefied area in order to judge whether a foundation will fail or survive. To describe the spatial pattern of liquefaction/non-liquefaction, we consider a binary random field, either 1 (liquefaction) or 0 (non-liquefaction), using a spatially correlated binary function. Two random field models are employed : (1) a spatially continuous model and (2) a spatially discrete model. The former model generates the safety margin[2] in space for a given fraction of liquefied area[3]. A negative safety margin indicates the occurrence of liquefaction, whereas a positive safety margin means the non-occurrence. The stability of the foundation is judged in each simulation of safety margin considering the simulated distribution of liquefied area and the failure criteria applicable to the foundation. A number of simulation trials enable us to obtain the conditional failure probability of the foundation given a fraction. In the case when the fraction of liquefied area is uncertain, the failure probability is calculated from the conditional probabilities of all the possible fractions and their probability density. In this model, the spatial dependence in the safety margin is taken into account in the form of a correlation distance. As an alternative, a spatially discrete (autoregressive) model is used to directly represent the spatial distribution of

---

[2] (Safety Margin) = (Soil Resistance) - (Earthquake Load)

[3] (Fraction of the liquefied area) = (Area of the liquefied region)/(Total area of the site)

liquefaction. A set of autoregressive coefficients express the degree of spatial dependence. The basic procedure for evaluating the failure probability is the same as that mentioned for the spatially continuous model.

To summarize, the main point of this research is to establish a methodology to evaluate the safety of foundations against liquefaction. A discussion about model input parameters, such as the fraction of liquefied area and autoregressive coefficients, are found in other research (e.g. Liao (1986)).

The thesis is organized as follows.

Chapter II presents a brief review of previous studies regarding the methods of liquefaction evaluation. The deterministic methods, and the probabilistic and statistical methods are reviewed.

In Chapter III, the problem considered in this study is described and a general approach is presented. Foundations are classified according to shape and size, and criteria for evaluating their stability are given. A large footing, such as the foundation of an oil tank, and scattered footings of building foundations are examples of different types. The vertical extent of liquefaction will occasionally be a problem in deep foundations, especially for structures supported by piles.

Chapter IV considers the liquefaction evaluation before discussing the spatial distribution of liquefied area. We introduce the fraction of liquefied area to total area. This quantity is used as a basis in simulating the spatial distribution of liquefied area. In addition, its variability and influential factors are briefly discussed.

Chapter V describes a methodology to evaluate the probability of foundation failure. Two alternative random models are employed: (1) the spatially continuous model and (2) the spatially discrete model, so that we simulate the spatial distribution of liquefied area, taking into account the correlation and uncertainties in soil resistance and

earthquake load. In the spatially continuous model, we introduce the concept of a safety margin. From the simulation of safety margins, a possible distribution pattern of liquefaction is obtained. Alternatively, the spatially discrete model generates a possible distribution pattern for a given fraction of liquefied area and a given set of autoregressive coefficients. A number of simulations of distribution pattern give the conditional failure probability given the fraction of liquefied area. The probability of foundation failure is calculated based on the conditional failure probability and the uncertainty of the fraction.

Chapter VI deals with some simplified but important problems to illustrate the proposed methodology. For a one-dimensional problem, the safety of two types of foundations, i.e. a single large foundation mat and a foundation made up of several scattered footings, is studied through numerical simulation. As for two-dimensional problems, simulations of the spatial distribution of liquefaction are presented. The results of simulations are examined and a comparison of the two models is made.

Conclusions and recommendations for future work are stated in Chapter VIII.

CHAPTER II. REVIEW OF STUDIES ON LIQUEFACTION EVALUATION

2.1 Overview

Figure 2.1 presents the currently available methods of liquefaction evaluation. They are classified into two groups: 1) the deterministic methods and 2) the probabilistic and statistical methods. The deterministic methods either determine the occurrence of liquefaction or give an answer in the form of a safety factor, while the probabilistic and statistical methods take into account a variety of uncertainties in the following areas :

1) magnitude and location of earthquakes

2) acceleration and duration of ground shaking

3) basic physical models of soil liquefaction

4) soil resistance parameters input to the model

They give an evaluation of the liquefaction susceptibility in terms of probability.

Moreover, the deterministic methods are grouped into (1) the simplified methods and (2) the detailed methods. The simplified methods are based mainly on widely collected liquefaction/non-liquefaction records in past earthquakes and a number of laboratory tests. They construct the boundary between liquefaction and non-liquefaction, focusing on the critical characteristics of ground (e.g. soil properties, water table) and/or of earthquake (e.g. peak ground acceleration, duration of shaking). Four approaches are grouped in the simplified methods depending on which parameters are chosen (see Figure 2.1). On the other hand, the detailed methods deal with the theoretical behavior of soil subjected to shaking. Constitutive laws[1] and models expressing the buildup of pore-water pressure are employed to compute the soil behavior. Four approaches are presented depending on the interpretation of stress (total stress or effective stress) and drained or

---

[1] Relationships between the stress and the strain of soil

undrained conditions.

The probabilistic methods deal with the conditional probability of liquefaction, given that an earthquake of specified location and magnitude or a ground shaking with specified acceleration and duration occurs. They involve the use of deterministic models to analyze for liquefaction at a site, estimating the inherent uncertainties in the characteristics of ground and earthquake. The statistical methods deal with how to draw the best boundary separating field observations of liquefaction and non-liquefaction records. The objective of the statistical methods is to extract useful information from data in terms of probability.

Each method of liquefaction evaluation mentioned above will be briefly discussed next.

2.2 Deterministic Methods

Simplified Methods

Simple geotechnical criterion

Kuwano (1992) evaluated liquefaction susceptibility at a given site using the grain size characteristics or fine content. The critical N-value method, in which the N-value is related to depth or maximum ground acceleration on the basis of several liquefaction records, is also one of the simplest criteria. Because of their low accuracy, these methods are commonly used only in a primary evaluation stage to determine whether or not a layer will be susceptible to liquefaction. Thus, more detailed evaluation methods need to be used in actual design projects.

15

Stress-based approach

A number of field observation data form a basis for establishing empirical correlation relating the occurrence and non-occurrence of liquefaction. This approach is basically the comparison of the soil resistance to the intensity of ground motion. The former is represented by a function of the N-value which is based on field experience during actual earthquakes and a number of laboratory tests, and the latter is the ratio of the average peak shear stress to the initial vertical effective stress. The ratio between such resistance and load variables is called the liquefaction resistance factor F_L. The effects caused by (1) the irregularity of earthquake motion, (2) the duration of the ground shaking corresponding to the magnitude of the earthquake, and (3) the prevailing period of the earthquake are taken into account by correction coefficients in order to simplify the model. This approach can be traced back to Seed and Idriss (1971). Many researchers have improved their original criterion as more data have become available and as the interpretations of the data have been refined. The criteria proposed by Iwasaki and Tatsuoka (1978), Tokimatsu and Yoshimi (1983), and Seed et al. (1985) are this type and are widely used in practice. Iwasaki and Tatsuoka added medium grain size D_{50} as an explanatory variable in the resistance term to the Seed and Idriss model (1971), and they also modified the correlation factors based on their laboratory tests. Tokimatsu and Yoshimi employed fine content (FC) in place of medium grain size. Seed and Idriss revised the measured SPT N-value and introduced another coefficient in the resistance term to modify the earthquake magnitude.

This approach has two problems in the evaluation of model input parameters :

(1) the uncertainty[2] in measured N-value and (2) the difficulties of performing enough

---

[2] It is a widely known fact that the measurement of SPT N-value depends greatly on who measures it and how it is measured.

number of SPT and grading test regarding cost and time in actual projects. To overcome them, the shear wave velocity by means of the Spectrum-Analysis-of-Surface-Wave (SASW) method has been utilized. Since the SASW method is less dependent on the tester than the SPT and does not require bore holes, it is feasible in the field due to its low cost. It is also well-suited for hard-to-sample materials. There are two liquefaction assessment methods based on the shear wave velocity. The first one was proposed by Stokoe and et al. (1988). They evaluated the relationship between the shear wave velocity of the liquefiable layer and the peak ground surface acceleration causing initial liquefaction. The other method uses the stress-based criteria by converting the shear wave velocity into the equivalent N-value (Takaya et al., 1991). In this method, the critical shear wave velocity, which gives $F_L=1$, is compared with the measured shear wave velocity in the field in order to evaluate the liquefaction potential. In other words, liquefaction is assumed to occur when $Vs < Vs_{critical}$. Both methods show good agreement with previous research and with past liquefaction records. Another advantage is that we can construct the liquefaction potential map easily by means of the SASW method (Takaya et al., 1991).

The Cone Penetration Test (CPT) is also considered as a simpler and faster sounding method than SPT. Robertson(1986), Tanisawa and et al. (1988) investigated the relationship between the cyclic stress ratio (Seed and Idriss, 1985) and cone resistance.

Although the F_L value can give a liquefaction potential at an arbitrary point in a soil column, it does not indicate the spatial extent and degree of liquefaction severity, which are very important characteristics when dealing with spatially extended or distributed structures. Iwasaki et al. (1982) quantified its severity by the liquefaction potential index P_L expressed as:

$$P_L = \int_0^{20} (1 - F_L) (10 - 0.5z) \, dz \qquad (2.1)$$

where z : depth (m)

The liquefaction potential of a site is classified as no liquefaction ($P_L = 0$), minor liquefaction ($0 < P_L \leq 5$), moderate liquefaction ($5 < P_L \leq 15$), or major liquefaction ($15 \leq P_L$), respectively. Kishimoto (1989) and Ohtomo (1990) constructed the fragility curve, which gives probability of each degree of the liquefaction severity against peak ground acceleration, using this index.

Strain-based approach

Since the stress-based approach is concerned with the occurrence of initial liquefaction, it cannot predict the soil behavior subsequent to initial liquefaction. The strain-based approach, in which the liquefaction parameters include the strain amplitude and the number of cycles, encompasses the liquefaction process completely. Talagnov (1992) performed the cyclic strain tests, and concluded that the process of liquefaction develops even after the initial liquefaction and, in that phase, the pore-water pressure has a tendency of transforming from cyclic to a constant, while the shear resistance of the soil tends toward a complete reduction. No model for analysis has yet been developed at this stage.

Energy-based approach

This approach is relatively new. The stress-based approach does not give accurate answers because:

1) the cyclic stress ratio depends on the type of loading and the correction coefficients for irregular loading contains a certain degree of error

18

2) it does not directly deal with the ratio of the pore-water pressure to the effective

overburden stress

The energy-based approach will serve as a general and rational alternative to the stress-based approach. The procedure uses a nearly unique relation between the pore-water pressure and the absorbed energy, which meets the basic mechanism of liquefaction. Two studies should be mentioned. One is an experimental approach studied by Kagawa (1988). The other is a theoretical approach done by Igarashi (1992).

Kagawa (1988) established two relationships based on laboratory tests and past liquefaction records: 1) a relationship between pore-water pressure and normalized energy, and 2) a relationship between maximum ground acceleration and normalized energy. Once a design earthquake is given, the liquefaction potential can be estimated by using one of these relationships.

Igarashi (1992) expressed the factor of safety against liquefaction as the ratio of the energy accumulated in the pore-water to the work (the elastic strain energy)[3] done to the pore-water by the ground motion during an earthquake. In calculating the latter one, he adopted the dislocation energy concept. Compared to the other method, his approach is so theoretical that it requires detailed information about ground motions, such as the RMS velocity and RMS acceleration of the earthquake, the strong motion duration, and the bandwidth index of the ground velocity. Judging from the rapid progress of experiment and observation apparatus, this method may come to be used as widely as the existing stress-based methods.

---

[3] The elastic strain density at pressure p can be $E = \frac{1}{2} n C p^2$, where n is the porosity and C is the compressibility of the pore-water.

Detailed Methods

The most important mechanism leading to liquefaction is the increment of pore-water pressure. In detailed evaluation methods, the pore-water pressure during earthquake motion is directly evaluated using numerical procedures. Four kinds of methods are listed in Figure 2.1. Roughly speaking, the analysis consists of two steps.

Step-1   Dynamic analysis to compute time histories of stress and/or strain within a soil mass.

Step-2   Computation of generation or dissipation of pore-water pressures

In D-1) and D-2) in Figure 2.1, these two steps are carried out separately, while they are performed simultaneously in D-3) and D-4) by taking the change of the pore-water pressure during cyclic loading into the stress-strain relationship (constitutive laws). This means that the effective stress analysis is superior to the total stress analysis in theory, and it also yields the deformation during the motion. However, there are two drawbacks in effective stress analysis :

1) the computer code tends to be very complicated

2) sophisticated engineering judgment is often necessary in defining the required material constitutive parameters from experiments

By contrast, the total stress analysis is easy to perform and can be interpreted in the same way with the stress-based F_L type analysis. At present, it is considered appropriate to use total stress analysis as a primary method and to use effective stress analysis if more detail evaluations are needed.

Many researchers have worked on improving the effective stress method. Prevost (1981) developed the finite element code called "DYNAFLOW" and Abe (1992) developed a code called "EFFECTD" for two- or three-dimensional problems by combining available constitutive models. Prevost (1992) also compared the numerical

results obtained by his code to experimental results, which confirms the validity of his approach. Incidentally, "SHAKE", "FLUSH" and "MASH" are often used for the total stress method, while "DESRA", "APOLLO" and "YUSA-YUSA" are used for the effective stress method. Each code has merits and limitations. Currently, none is universally accepted . Further development may be expected in the near future. For example, Oka (1988) proposed an elasto-plastic model for sand, and an elasto-viscoplastic model for natural soft clay as a constitutive law in terms of shear deformation. Canou (1992) proposed the concept of collapse surface in (q, p', e) space, where static liquefaction is initiated.

2.3 Probabilistic and Statistical Methods

While the deterministic methods predict whether or not liquefaction will occur, probabilistic and statistical methods can assess liquefaction risk, which is the information needed for making decisions under uncertainty. Halder (1979) applied a first-order second-moment (FOSM) method to a deterministic method proposed by Seed and Idriss (1971). A more sophisticated approach was presented by Fardis and Veneziano (1982) to include the effects of pore-water pressure diffusion and soil stiffness reduction, and variation of soil properties within a stratum. Chameau (1983) proposed probabilistic analyses based on pore-water pressure generation models that is combined with a stochastic description of the earthquake motion. The accumulation of pore-water pressure is calculated using a nonlinear formulation. In either approach, distributions of load and resistance parameters are modeled as a certain distribution form in estimating the conditional probability of liquefaction.

21

Statistical methods deal with the extraction of information from past liquefaction/nonliquefaction records. Christian (1975), and Davis and Berrill (1982) used a method of statistical classification known as the linear discriminate analysis. Yegian and Whitman (1978) found the line that best separates liquefaction from non-liquefaction points by minimizing the sum of squared distances to the misclassified points. Liao (1986) used a method of statistical binary regression rather than classification to quantify the probability of liquefaction as a function of given parameters. This approach is illustrated here because it will be used later in this research. Liao developed statistical models to express the probability of liquefaction as a function of earthquake load and soil resistance parameters. Results were obtained based on 278 cases of historic data catalog concerning liquefaction/nonliquefaction occurrences. A method of binary regression, called logistic regression, was used to derive two types of models for use in the assessment of liquefaction probability. One of them, called the "local model," uses the cyclic stress ratio as the earthquake load parameter. Liao obtained the following equations :

$$P_{L|Q_L} = 1 / \{1 + \exp(-Q_L)\} \qquad (2.2)$$

where $P_{L|Q_L}$: conditional probability of liquefaction given $CSRN$ and $(N_1)_{60}$

$Q_L = 10.167 + 4.1933 \ln(CSRN) - 0.24375(N_1)_{60}$ (no differentiation between

clean and silty sand) (2.3)

$Q_L = 16.447 + 6.4603 \ln(CSRN) - 0.39760(N_1)_{60}$ (clean sand FC<12%) (2.4)

$Q_L = 6.4831 + 2.6854 \ln(CSRN) - 0.18190(N_1)_{60}$ (silty sand FC>12%) (2.5)

$CSRN$: normalized cyclic stress ratio

$(N_1)_{60}$: corrected SPT resistance

The other, so called "source model," uses explicit functions of earthquake magnitude and distance as load parameters. In this case, $P_{L|Q_L}$ is the same as the above, with Q_L given by:

$$Q_L = -12.922 + 0.87213 \ln(\Lambda_{EP}) - 0.21056(N_1)_{60} \tag{2.6}$$

$$Q_L = -15.143 + 1.0837 \ln(\Lambda_{HY}) - 0.22656(N_1)_{60} \tag{2.7}$$

where $\Lambda_{EP}, \Lambda_{HY}$: earthquake-load functions

$$\Lambda_{EP} = \frac{10^{1.5M}}{(R_{EP})^2 (\overline{\sigma}_v)^{1.5}}, \quad \Lambda_{HY} = \frac{10^{1.5M}}{(R_{HY})^2 (\overline{\sigma}_v)^{1.5}} \tag{2.8}$$

M : Richter magnitude

$\overline{\sigma}_v$: effective vertical stress (kg / cm^2)

R_{EP} : epicentral distance (km)

R_{HY} : hypocentral distance (km)

An advantage of this method is that the probability distribution of soil resistance parameter (i.e. $(N_1)_{60}$) and earthquake load parameters (e.g. $CSRN$) do not need to be estimated. That is, the conditional probability for a given soil resistance parameter and earthquake parameters is directly evaluated.

23

Deterministic Methods

Simplified methods

S-1) Simple geotechnical criterion : simple but less reliable, a primary evaluation

S-2) Stress-based approach : widely used both in research and in practical design projects

S-3) Strain-based approach : evaluation for post-liquefaction

S-4) Energy-based approach : new

Detailed methods

D-1) Undrained total stress analysis : relatively simple

D-2) Partially drained, total stress analysis

D-3) Undrained effective stress analysis

D-4) Partially drained, effective stress analysis   : very complicated but superior to the
                                                          others in theory

Probabilistic and Statistical Methods

Probabilistic methods : randomness in earthquake and uncertainties
                         in soil properties are taken into account

Statistical methods : the best boundary separating field obsevations of
                       past records are sought

Figure 2.1 Classification of Methods on Liquefaction Evaluation

CHAPTER III.   PROBLEM DEFINITION AND GENERAL APPROACH

3.1 Problem Definition

It is clear that the size and shape of liquefied areas vary in the horizontal geographical plane and in depth. Sometimes large isolated liquefied areas are observed, while in others many small liquefied regions may be seen. Even if one knows the mean value of the soil resistance to liquefaction and the earthquake load at a site so that the fraction of liquefied area to total area can be somehow evaluated, the spatial distribution of liquefied area will still vary in a manner which is hard to predict. The spatial distribution of liquefied area greatly depends on the horizontal and vertical correlation in soil resistance such as soil properties and water table, and in earthquake load such as the magnitude and peak ground acceleration. Although it is extremely hard to reveal their correlation structures accurately, predicting the distribution of liquefied region is crucially important to evaluate the safety of laterally extended foundations that are constructed on the liquefiable ground.

Moreover, the safety of foundations is concerned with the criterion applied to the foundation regarding its stability. A big foundation, such as the foundation of an oil tank, may have a criterion totally different from that of small foundations such as footings of a building. In the former foundation, the size of liquefied region beneath the foundation may be a problem, while the location of liquefied region may be critical in the latter. Therefore, the safety of foundations has to be examined in association with the type of foundation and their vulnerability as a function of the spatial and vertical pattern of liquefaction, which is discussed in this chapter. The following three types in Table 3.1 are considered.

25

Table 3.1 Types of Foundation and the Liquefied Region

Type	Main concern	Structures
Type-A	Extent of liquefied region	a tank foundation, an underground pipeline
Type-B	Location of liquefied region	footings of building and bridges towers of power cables
Type-C	Vertical extent of liquefied layer	an offshore platform supported by piles

Figures 3.1 and 3.2 are provided as references regarding the distribution pattern of liquefaction and the possible failure mode of each structure.

Type-A

The foundations belonging to Type-A lose their stability when the liquefied region beneath the foundation is larger than the area necessary to support the structure. The size of the liquefied region is of primary concern. The failure probability P_f can be expressed as :

$$P_f = P [A_L > A_n]$$

(3.1)

where A_L : area of liquefied region

A_n : area of non-liquefied ground needed to support the superstructure.

In general, the degree of damage will depend on the size of liquefied region.

Type-B

A building is usually supported by many footings, which are connected to columns. Often, the area of each footing is not large. However, liquefaction under any footing may result in serious damage or even collapse of the structure. In this case, we must be concerned with the location of liquefied region rather than the extent of such region. The failure probability is as follows :

$$P_f = P [A_f \subset A_L] \tag{3.2}$$

where A_f : location of non-damage footings needed to support the

superstructure

A_L : location of liquefied region

Note that " A ⊂ B" denotes A encompasses B.

Type-C

Up to now, we have considered the lateral extent of liquefaction. Indeed for shallow foundations, the thickness of the liquefied layer is of secondary importance. However, such thickness may greatly affect the stability of deep foundations. Consider, for example, an offshore platform supported by piles. If liquefaction with a certain thickness occurs, we cannot count on the lateral resistance provided by the liquefied soil. This situation may cause failure of the piles and excessive lateral deformation because of the increased free length of the piles above the embedded part. In foundations of Type-C, the thickness of the liquefied layer affects the behavior of the foundation in terms of its stability. Hence,

$$P_f = P [L_L > L_N] \tag{3.3}$$

27

where L_L : thickness of liquefied layer

             L_N : length to be embedded into the ground needed to support the

             superstructure

The above classification is very schematic. The safety of actual foundations engineers deal with is controlled by many factors. One may sometimes encounter a situation where controlling factors need to be combined. In reality, both lateral and vertical extent may be important.

3.2 General Approach

Type-A and Type-B foundations are sensitive to the horizontal distribution pattern of liquefied area, while Type-C is concerned mainly with the vertical extent. In this research, the safety of Type-A and Type-B foundations is studied, and that of Type-C foundation will remain a future task. Thus, our goal is to estimate the spatial distribution pattern of liquefied area in terms of its extent and location, and to evaluate the safety of foundations in terms of probability.

Figure 3.3 shows the general approach employed here, which consists of five steps. Each step is briefly described.

Step-I

Liquefaction depends on many characteristics of ground such as soil strength, soil type, grain size, age, water table. It is necessary to choose the most critical property of ground among the available sounding data. N-value is widely used in the evaluation methods of liquefaction, and superior to other parameters with respect to availability. In order to mathematically characterize a given ground, the distribution of soil properties as well as their correlation needs to be investigated.

Step-II

As parameters of earthquake loads, either M and R in the source model or PGA and duration of shaking in the local model may be utilized. The choice of parameters depends on the method used to evaluate the liquefaction susceptibility. PGA, for example, will be used if the possibility of occurrence is estimated by the Seed-Idriss model (1985). It is possible to combine them, that is, we can evaluate the probability of liquefaction based on the PGA that is obtained from M and R by using an attenuation equation. In this research, the local model is employed. The variability in PGA should be taken into consideration similarly in Step I.

Step-III

Before considering the spatial distribution pattern of liquefied area, we need to specify the fraction of liquefied area, which is used later. It may be estimated by assessing uncertainty in influential factors to liquefaction or statistical analysis of damage reports (observed data) recorded in the past earthquakes. However, since characteristics of ground and earthquake differ from earthquake to earthquake, and most of the reports have not stated the liquefied area accurately due to the difficulty in its survey, we cannot utilize these means. Therefore, we estimate the expected value of the fraction based on results in Liao (1986), and we determine some mathematical form judgmentally to express the variability of the fraction in the case when the fraction is uncertain. A detailed discussion will follow in Chapter V.

Step-IV

The spatial correlation in soil resistance and earthquake load has to be taken into account in order to simulate the spatial distribution pattern of liquefied area. Two

29

alternative random models are employed as mentioned before: (1) the spatially continuous model and (2) the spatially discrete model.

In the approach based on the spatially continuous model, first, we introduce a concept of safety margin (SM), which is equal to the soil resistance minus earthquake load. A negative value of the safety margin means that liquefaction will occur, while a positive value means that liquefaction will not. We assume that the safety margin is a Gaussian random field. The ratio of the area where safety margin is smaller than zero to total area corresponds to the fraction of liquefied area discussed in the previous step. The simulation of the safety margin is performed on the basis of the spatially continuous model, in which the correlation is expressed in the form of a correlation distance. The mean value and the standard deviation of the safety margin are necessary for the simulation. The mean value is determined in terms of the fraction of liquefied area obtained in Step-III, and the standard deviation is assumed without loss of generality.

In the spatially discrete model based approach, the occurrence of liquefaction at a point depends on the fraction of liquefied area and the information at adjacent points expressed in the form of a binary variable (0: non-liquefaction, 1: liquefaction). The correlation structure is expressed by the autoregressive coefficients.

Step-V

A single simulation performed in the previous step can only give a possible distribution pattern of liquefaction, and it cannot be interpreted as a deterministic answer. Instead, a number of simulation results enable us to obtain a conditional failure probability given a fraction on liquefied area. That is, in every simulation, we judge whether the foundation will fail or survive in consideration of the simulation result and the design criterion applicable to the foundation concerning its stability. By dividing the
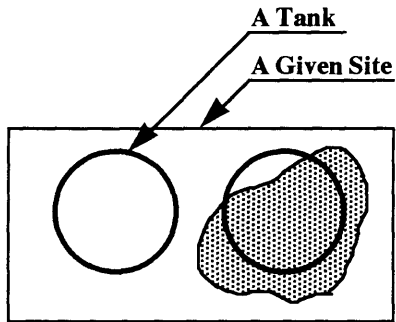
30

total number of simulation trials by the number of "fail" trials, we can obtain the conditional failure probability of the foundation for a given fraction. In the case when the fraction has some variability, we need to perform this simulation for all the fractions to obtain the failure probability. More details will be presented in Chapter-V.

In summary, the three important factors influencing the failure probability of foundations are as follows :

　　1) the fraction of liquefied area and its variability (Step-III)

　　2) the spatial variation of liquefied area (Step-IV)

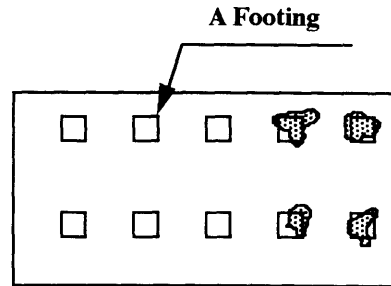　　3) the vulnerability of foundations (Step-V)

These are combined and taken into account in the proposed methodology. In the next chapter, we consider the fraction of liquefied area and its variability, which are followed by a discussion on the other two factors.
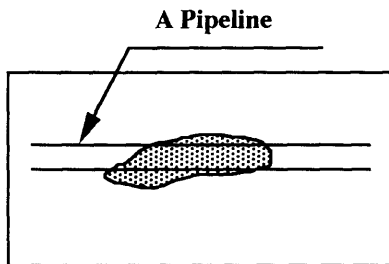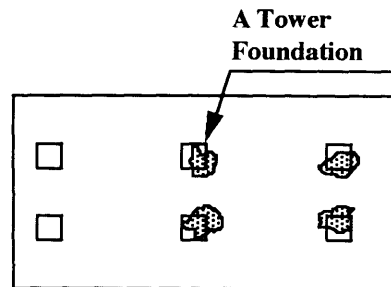
Type A

A Tank

A Given Site

Tank Foundations

A Pipeline

An Underground Pipeline

Type B

A Footing

Footings of A Building

A Tower Foundation

Towers of Power Lines

Type C

increased
free length

Sea bed

A Pile

An Offshore Platform
(Elevation)

Legend

: Liquefied Area

Figure 3.1 Distribution Patterns of Liquefied Region

32

Type A

Tank Foundations

Type B

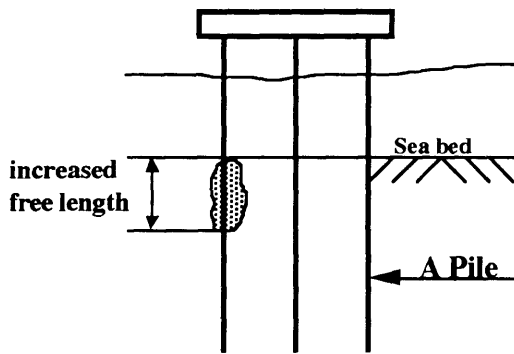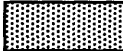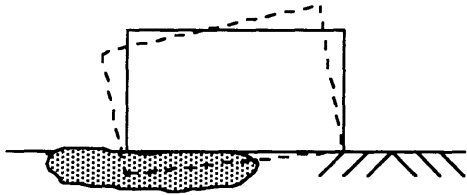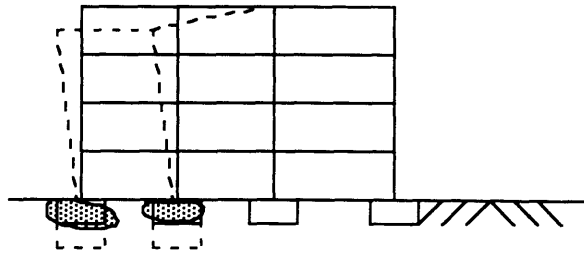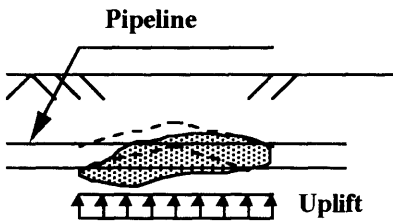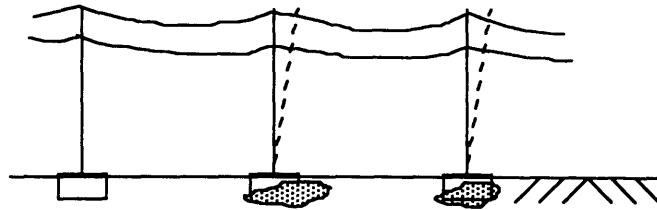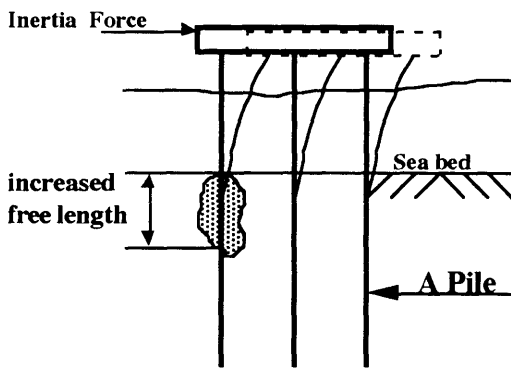**Footings of A Building**

An Underground Pipeline

Towers of Power Lines

Type C

An Offshore Platform
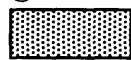
Legend

 : Liquefied Area
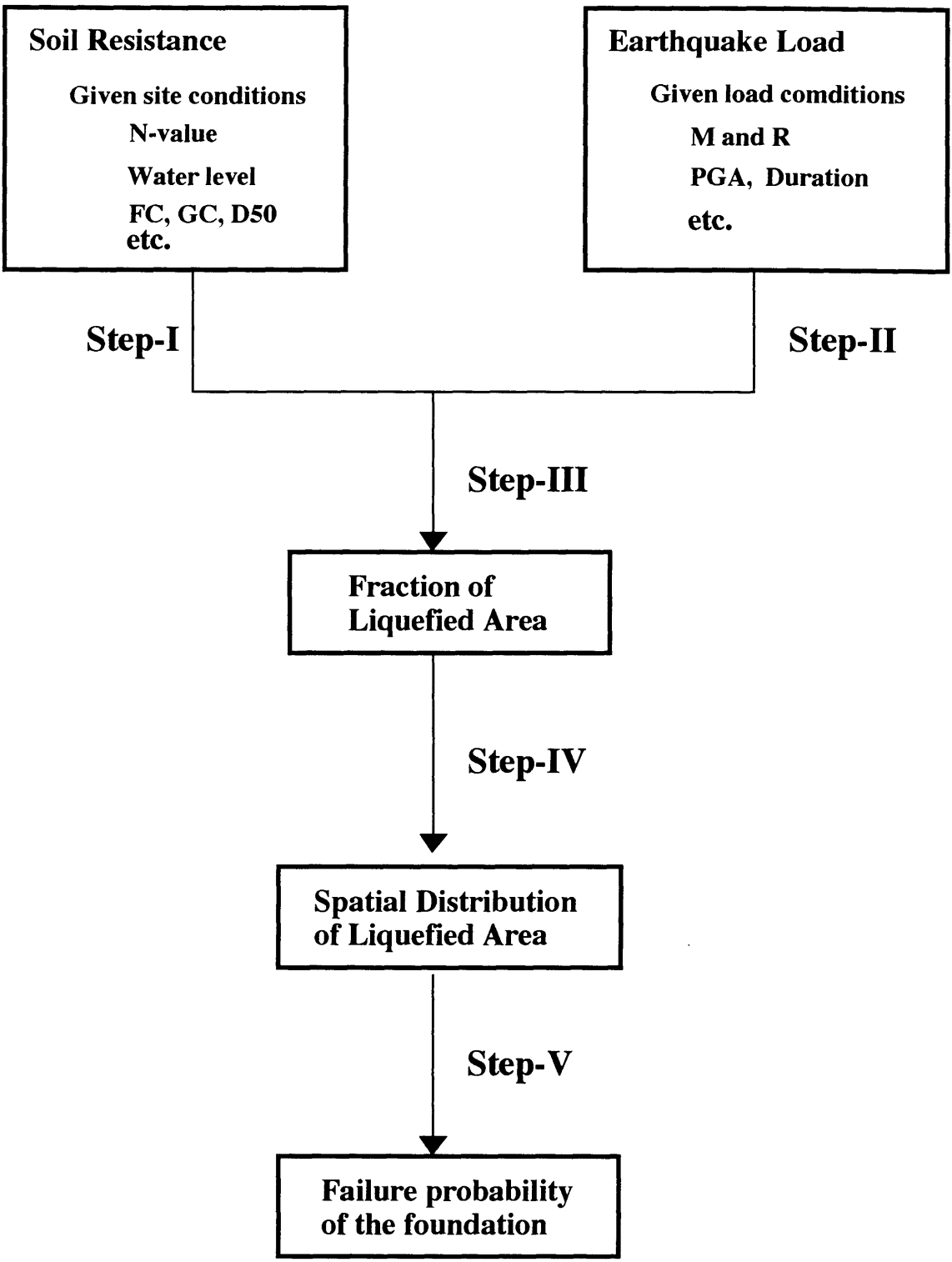
Figure 3.2 Failure Modes

33

Figure 3.3 General Approach

CHAPTER IV.   EVALUATION OF THE FRACTION OF LIQUEFIED AREA

As mentioned in the previous chapter, the fraction of liquefied area[1] must be examined first before investigating the spatial distribution of liquefied area.

4.1 Definition of the Fraction of Liquefied Area

The fraction of liquefied area, γ , is defined as :

$$\gamma = \frac{A_L}{A} \tag{4.1}$$

where A :   area of region around the site with statistically homogeneous soil

properties and statistically homogeneous ground shaking

A_L :   area of liquefied subregion $(= \sum A_i$, see Figure 4.1)

One of the characteristics of the fraction γ is that, for a given region, the fraction γ varies not only with M and R but also from earthquake to earthquake. In addition, the fraction γ varies from site to site for a given earthquake (e.g., a given set of M and R). Because of their variability, it would be inappropriate to deal with the fraction γ as a deterministic quantity. Influential factors to the fraction of liquefied area will be discussed next and then the variability of the fraction γ will be examined.

4.2 Influential Factors to the Fraction of Liquefied Area

The liquefaction potential of a soil deposit depends on a combination of soil properties, geologic factors and characteristics of the earthquake to which the deposit is subjected.   Seed and Idriss (1982) indicate the following as important factors in

---

[1] The fraction of liquefied area is equivalent to the liquefaction probability in the site with statistically homogeneous soil properties and statistically homogeneous ground shaking.

35

evaluating liquefaction potential. The factors with an asterisk are used in the deterministic methods, either directly or in modified form.

Soil Properties:
        Dynamic shear modulus
        Damping characteristics
        Unit weight*
        Grain characteristics* (median grain size, fine content, gravel content)
        Relative density*
        Soil structure

Geologic Factors:
        Method of soil formation
        Seismic history
        Geologic history (aging, cementation)
        Depth of water table*
        Effective confining pressure

Earthquake Characteristics:
        Intensity of ground shaking*
        Duration of ground shaking*

Yasuda (1988) added some other factors :

Soil Properties:
        Plasticity index
        Degree of saturation

Geologic Factors:
        Anisotropy of stress
        Initial shearing stress
        Over consolidation ratio
        Time of consolidation

36

Earthquake Characteristics:

Direction of shaking

Shape of shaking wave

Drain condition

Others:

Degree of disturbance of test specimen

Test equipment

The fact that all of the factors listed above are involved complicates the evaluation of the liquefaction potential at a site. Some factors have a great impact on the liquefaction potential, while others do not.

4.3 Expected Fraction of Liquefied Area

It is difficult to predict the fraction γ because of the complexity of its dependence on many unknown factors. Instead, we can estimate the expected fraction of liquefied area using results in Liao (1986). Liao developed statistical models to express the probability of liquefaction as a function of soil resistance and earthquake load parameters on the basis of 278 cases of liquefaction and non-liquefaction occurrences. Four liquefaction probability models were derived through binary regression analysis. The probability obtained by these models will be used here as the expected fraction of liquefied area. The following logistic equation is adopted here (see Figure 4.2).

$$E [\gamma] = E [P_{L|Q_L}] = \frac{1}{\{ 1 + \exp (-Q_L) \}} \tag{4.2}$$

$$Q_L = 10.167 + 4.1993 \ln (CSRN) - 0.24375 (N_1)_{60} \tag{4.3}$$

37

where $P_{L|Q_L}$: conditional liquefaction probability for a given Q_L that

is a function of $CSRN$ and $(N_1)_{60}$

$CSRN$: the normalized cyclic stress ratio,

$(N_1)_{60}$: the corrected/normalized blow count

Figure 4.3 shows the relationship between CSRN and the expected fraction γ for different values of the blow count number. In this case, a magnitude $M = 7.5$, depth $z = 0$, and ratio of total stress to effective stress $r = 0$ are assumed. If soil properties and earthquake characteristics are different from these, the curves will change.

4.4 Variability of the Fraction of Liquefied Area

Figure 4.3 shows only the expected value of the fraction of liquefied area. However, the fraction γ will display some variability both from site to site and from earthquake to earthquake around this expected value. Site-to-site variability is due mainly to the variability of soil properties. For example, the grain size distribution and the geologic history of the site are not entirely determined by $CSRN$, $(N_1)_{60}$, and the soil class should be expected to have some residual effect on the fraction γ. Earthquake-to-earthquake variability is due mainly to the variability of the intensity and duration of ground shaking.

The variability of the fraction of liquefied area could be evaluated in different ways :

(1) by considering the effect of other influential factors, assessing uncertainty in the factors, and propagating the uncertainty,

(2) by using historical liquefaction data reported in terms of the fraction γ, or

(c) judgmentally.

Since the effects of all influential factors needed in Approach (1) are not well known and the historical data required by Approach (2) is also unavailable, here we follow Approach (3) and express the distribution of γ based on engineering judgment. The fraction of liquefied area must take some value between 0 and 1 : γ = 0 means that liquefaction will not occur anywhere in the region and γ = 1 indicates that the entire area under consideration will liquefy. A convenient model to represent uncertainty in γ is the Beta distribution (see Figure 4.4). In terms of the mean value and variance, the density of the Beta distribution is :

$$f_x(x) = \frac{1}{B} x^{r-1} (1-x)^{t-r-1} \quad (0 \leq x \leq 1) \tag{4.4}$$

where the normalizing constant is :

$$B = \frac{(r-1)! \, (t-r-1)!}{(t-1)!} \tag{4.5}$$

The mean and variance of the distribution are :

$$m_x = \frac{r}{t} \tag{4.6}$$

$$\sigma_x^2 = \frac{m_x \, (1 - m_x)}{t+1} = \frac{r \, (t-r)}{t^2 \, (t+1)} \tag{4.7}$$

We need to estimate the mean and variance to specify the density of the Beta distribution. The mean can be determined using results in Liao (1986) as discussed in the previous section. Also, the variance could be estimated following three approaches mentioned earlier in this section.

39

So far we have considered the variability of the fraction of liquefied area. In order to evaluate the safety of foundations, we also need to know the spatial variation of the liquefied area (see Chapter III). A discussion of methods to represent and simulate the spatial variation of liquefied areas for a given fraction γ is given in the next chapter.
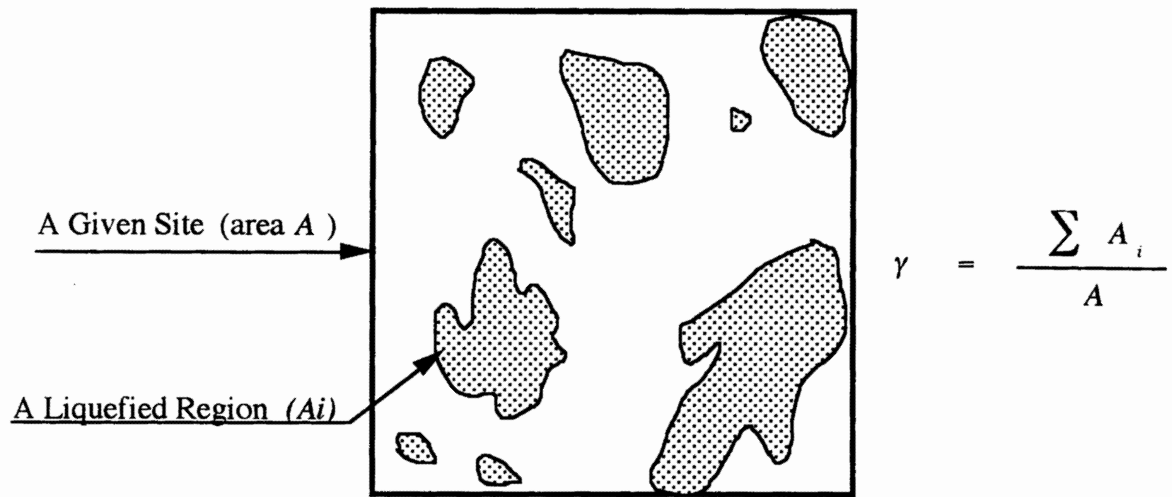
$$\gamma \quad = \quad \frac{\sum A_i}{A}$$

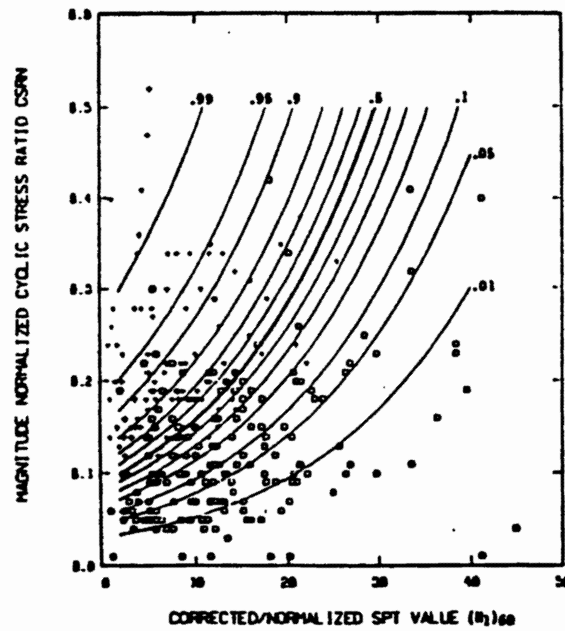Figure 4.1 Fraction of Liquefied Area[2]

Figure 4.2 Contour Lines of Equal Probability of Liquefaction[3]

---

[2]The given site has statistically homogeneous soil properties and statistically homogeneous ground shaking.
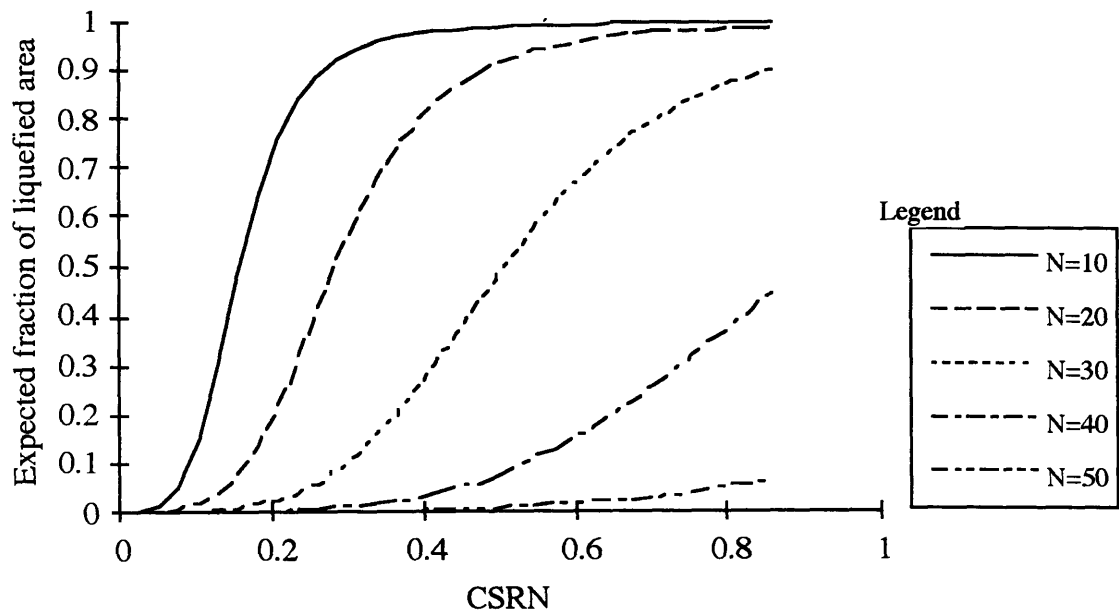[3]Derived from S. Liao (1986).

41

Figure 4.3 Relationship between CSRN and the Expected
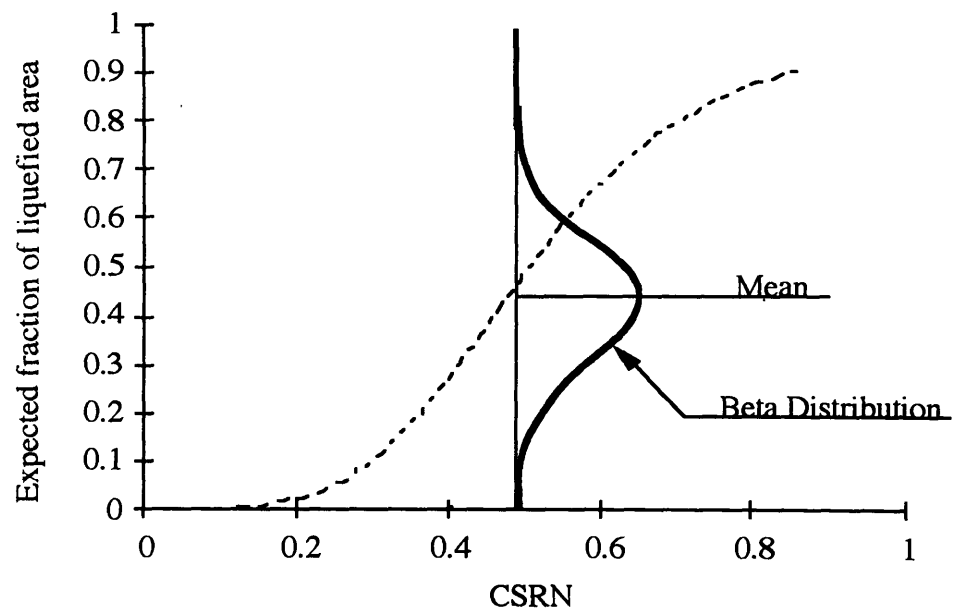Fraction of Liquefied Area[4]

Figure 4.4 Variability of the Fraction of Liquefied Area

---

[4] The fraction of liquefied area is equivalent to the liquefaction probability.

CHAPTER V.   SPATIAL DISTRIBUTION OF LIQUEFIED AREA AND PROBABILITY OF FOUNDATION FAILURE

5.1 General Description

As discussed in Chapter III, in order to evaluate the state of failure or survival of a foundation, we need to know the spatial distribution of liquefied area. For this purpose, we introduce an indicator random field Z (x, y), defined as follows :

$$Z(x, y) = \begin{cases} 1 : & \text{If liquefaction occurs at location } (x, y) \\ 0 : & \text{otherwise} \end{cases} \tag{5.1}$$

One property of the function Z (x, y) is that :

$$E[Z(x, y)] = \gamma = P_L \tag{5.2}$$

where γ : fraction of liquefied area

P_L : liquefaction probability

The liquefaction potential depends on the soil resistance and earthquake load, both of which have, in general, some degree of spatial correlation. This spatial correlation should be reflected in spatial dependence for the random field Z (x, y).

The spatial variation of liquefied area for a given value of the fraction γ is represented here by two alternative random models, which we refer to as : (1) the spatially continuous model, and (2) the spatially discrete model. These models and their properties are presented first and then their application to the problem of liquefaction risk is discussed.

In the spatially continuous model, we consider a level-crossing problem of continuos random function to generate the correlated 0-1 patterns of Z (x, y). We

introduce the concept of a safety margin, SM, defined as follows :

$$SM\ (x,\ y)\ =\ R\ (x,\ y)\ -\ L\ (x,\ y) \tag{5.3}$$

where $SM\ (x,\ y)$: safety margin at location $(x,\ y)$

$R\ (x,\ y)$: measure of soil resistance

$L\ (x,\ y)$: corresponding measure of earthquake load

Here, we assume that a random field $SM\ (x,\ y)$ is Gaussian. The indicator random function $Z\ (x,\ y)$ is related to the safety margin $SM\ (x,\ y)$ as :

$$
\begin{aligned}
Z\ (x,\ y)\ &=\ 1 \qquad wherever \quad SM\ (x,\ y)\ \leq\ 0 \\
Z\ (x,\ y)\ &=\ 0 \qquad wherever \quad SM\ (x,\ y)\ >\ 0
\end{aligned}
\tag{5.4}
$$

Figure 5.1 illustrates this relation in a one-dimensional case. Simulation procedures for the safety margin are discussed in APPENDIX. A detailed description of the spatially continuous model will follow in Section 5.2.

As an alternative to the spatially continuous model, we can employ a spatially discrete model, which gives a direct discrete representation of the pattern of liquefaction or non-liquefaction. Discretizing a given space into a rectangular grid, we assign a value either 1 (liquefaction) or 0 (non-liquefaction) to each grid point using the autoregressive model. Figure 5.2 shows the scheme of generating the 0-1 patterns of $Z\ (x,\ y)$ in a one-dimensional problem. A set of autoregressive coefficients, which express the spatial correlation of liquefaction potential, and the fraction of liquefied area is necessary for the completion of this model. Section 5.3 describes this model in detail.

5.2 Spatially Continuous Model

The spatially continuous model is used to represent the spatial variation of the safety margin which, through its region, gives information concerning the occurrence of liquefaction.

Generation of the Safety Margin (SM)

Since we assumed that the safety margin is a Gaussian random field, complete characterization of SM (x, y) requires the following parameters :

1) Mean value

2) Variance (or standard deviation)

3) Correlation function

The zero-crossing set of a safety margin does not depend on the magnitude of the variance, which acts simply as a scaling factor (see Figure 5.3). Thus, we assume without loss of generality that the variance is 1. Accordingly, the mean value m_{SM} must satisfy :

$$1 - \gamma = \Phi (m_{SM}) \tag{5.5}$$

thus,

$$m_{SM} = \Phi^{-1} (1 - \gamma) \tag{5.6}$$

where Φ : the standard normal CDF (see Figure 5.4)

The character of the spatial variation of liquefied and non-liquefied area depends on the correlation function, which in the case of isotropic variation is a function ρ (r) [1] of the separating distance r. Here, we employ the exponential correlation model :

---

[1] Since we already assumed that the variance of the safety margin is equal to one, the correlation function is equivalent to the covariance function (see Equation (A.8) in APPENDIX).

$$\rho \ (r) \ = \ e^{-(r/r_0)} \tag{5.7}$$

where r_0 : correlation distance

The smaller the correlation distance is, the closer to white noise the simulated safety margin becomes. Conversely, the greater the distance is, the less fluctuation the simulated safety margin shows.

Once the fraction γ and correlation distance r_0 are given, we can under the above assumptions simulate the safety margin process. A basic procedure to do so is described in APPENDIX.

Numerical Simulation for Evaluating the Failure Probability

As mentioned before, the fraction γ is often highly uncertain, even for given values of $CSRN$ and $(N_1)_{60}$. Therefore, the failure probability of the foundation given $CSRN$ and $(N_1)_{60}$ is expressed as :

$$P_f \ (\ CSRN, \ (N_1)_{60}) \ = \ \int_\gamma P_{f|\gamma} \ f_\gamma (\ \gamma \ | \ CSRN, \ (N_1)_{60} \ ) \ d\gamma \tag{5.8}$$

where $\qquad P_{f|\gamma}$: conditional probability of the foundation failure given γ

$f_\gamma (\gamma \ | \ CSRN,(N_1)_{60})$: probability density function of the fraction γ for a given $CSRN$

and a given value of the modified blow count number $(N_1)_{60}$

The probability density function $f_\gamma (\gamma \ | \ CSRN, \ (N_1)_{60})$ can be estimated as discussed in Chapter IV. However, since the vulnerability differs from foundation to foundation[2], it is impossible to give a general expression for the conditional failure probability $P_{f|\gamma}$. It is

---

[2] Foundations vary in size and shape, and failure criteria depend on the type of structure.

46

also typically difficult to obtain analytical results for any given system. Therefore, we rely on numerical simulation.

The basic procedure for evaluating the probability of foundation failure for a given γ is summarized below.

Step-1　Define $f_\gamma(\gamma \mid CSRN,(N_1)_{60})$ and correlation distance r_0 [3]

Step-2　Discretize $f_\gamma(\gamma \mid CSRN,(N_1)_{60})$ and set $\gamma = \gamma_i$ ($i = 1, \cdots , n$) [4]

Step-3　Compute the mean value m_{SM} for the given γ by Equation (5.6)

Step-4　Generate a safety margin at every point (see APPENDIX)

Step-5　Assign liquefaction or non-liquefaction to every point by Equation (5.4) based on the results in Step-4

Step-6　Determine the stability of the foundation, considering the design criteria applicable to the foundation

Step-7　Assign a binary value either P = 1 (failure) or P = 0 (non-failure)

Step-8　Iterate Steps -4 to -7 a number of times

Step-9　Take the mean of P as the conditional failure probability given γ_i $(= P_{f|\gamma_i})$

Step-10　Iterate from Step-2 through Step- 9 for all n

Step-11　Calculate the failure probability of the foundation by Equation (5.8) $(= P_f)$

The evaluation of the conditional failure probability $P_{f|\gamma}$ is exemplified in Chapter VI for some simple problems.

---

[3] The correlation distance r_0 is determined either by statistical means or judgmentally

[4] $f_\gamma(\gamma \mid CSRN,(N_1)_{60})$ is discretized into n portions. γ_i is the representative value of i-th portion.

5.3 Spatially Discrete Model

As an alternative, we may use a discrete autoregressive model to describe directly the spatial variation of $Z(x, y)$. Honjo (1985) has described some binary models, including autoregressive models.

Basic Model

The homogeneous autoregressive model derived by Bartlett and Besag (1969) on a rectangular grid has the property that (see Figure 5.5):

$$E [x_{ij} \mid x_{i-1,j}, x_{i,j-1}] = \alpha + \frac{1}{2} (\beta_1 x_{i-1,j} + \beta_2 x_{i,j-1}) \qquad (5.9)$$

where x_{ij} : binary random variable (i.e. 1 or 0)

α, β_1, β_2 : autoregressive coefficients.

All the autoregressive coefficients $(\alpha, \beta_1,$ and $\beta_2)$ are bounded between zero and one. Taking expectation,

$$E [x_{ij}] = \alpha + \frac{1}{2} (\beta_1 E [x_{i-1,j}] + \beta_2 E [x_{i,j-1}]) \qquad (5.10)$$

Under the condition of homogeneity, the expectation of x_{ij} is :

$$E [x_{ij}] = \gamma = const. \qquad (5.11)$$

So that, from Equation (5.10),

$$\gamma = \alpha + \frac{1}{2} (\beta_1 + \beta_2) \gamma \qquad (5.12)$$

Therefore,

$$\alpha = \left\{ 1 - \frac{1}{2}(\beta_1 + \beta_2) \right\} \gamma \qquad (5.13)$$

If β_1 and β_2 are estimated by either statistical or judgmental means and γ is given, we can obtain α from Equation (5.13). Substituting Equation (5.13) into Equation (5.9), the model is :

$$E [x_{ij} \mid x_{i-1,j}, x_{i,j-1}]$$

$$= \left\{ 1 - \frac{1}{2}(\beta_1 + \beta_2) \right\} \gamma + \frac{1}{2} (\beta_1 x_{i-1,j} + \beta_2 x_{i,j-1}) \qquad (5.14)$$

The autoregressive coefficients β_1 and β_2 give the one-step correlation of the process in each direction.

Application

We consider that x_{ij} takes a value of either 1 (liquefaction) or 0 (non-liquefaction). The fraction of liquefied area γ is obtained using results in Liao (1986). Thus, if the autoregressive coefficients are given, we can generate the probability of liquefaction at every point on the basis of the information from previous points in any direction. In this approach, the correlation with respect to liquefaction susceptibility among adjacent points is expressed by the autoregressive coefficients. If a high degree of correlation exists, greater coefficients would be chosen. Uncorrelated fields can be generated by assuming that the autoregressive coefficients are equal to zero.

Numerical Simulation for Evaluating the Failure Probability

The failure probability of a foundation given $CSRN$ and $(N_1)_{60}$ is expressed by Equation (5.8) in the case when the fraction γ is uncertain. A numerical simulation for evaluating the failure probability of a foundation is as follows.

In using this model, we discretize a given site into a rectangular $(m \times n)$ grid.

Step-1 Define $f_\gamma(\gamma \mid CSRN,(N_1)_{60})$ and β_1, β_2, m and n

Step-2 Discretize $f_\gamma(\gamma \mid CSRN,(N_1)_{60})$ and set $\gamma = \gamma_i$ ($i = 1, \cdots, n$)

Step-3 Simulate $x(1, 1)$:

      If a generated random number in $[0, 1] > \gamma$ [5], then $x(1, 1) = 0$

      Otherwise   , then $x(1, 1) = 1$

Step-4 Simulate the values of x_{ij} ($i = 1, \cdots, m$, $j = 1$) along the horizontal boundary based on the one-dimensional model :

$$P_{fH} = (1-\beta_1) \gamma + \beta_1 x(i-1, 1) \tag{5.15}$$

      If a generated random number in $[0, 1] > P_{fH}$, then $x(i, 1) = 0$

      Otherwise   , then $x(i, 1) = 1$

Step-5 Simulate the values of x_{ij} ($i = 1$, $j = 1, \cdots, n$,) along the vertical boundary using

$$P_{fV} = (1-\beta_2) \gamma + \beta_2 x(1, j-1) \tag{5.16}$$

      If a generated random number in $[0, 1] > P_{fV}$, then $x(1, j) = 0$

      Otherwise   , then $x(1, j) = 1$

---

[5] Since the liquefaction probability does not give a binary number either 0 or 1 directly, we make use of the Monte Carlo simulation, in which we compare the generated probability to a random number between 0 and 1.

Step-6   Simulate the values of x_{ij} ($i = 2, \cdots , m, \ j = 2, \cdots , n,$) in the interior

of the rectangle using

$$P_f = \left\{ 1 - \frac{1}{2}(\beta_1 + \beta_2) \right\} \gamma + \frac{1}{2} \left\{ \beta_1 x(i-1,j) + \beta_2 x(i,j-1) \right\} \quad (5.17)$$

If a generated random number in [0, 1] > P_f , then $x(i,j) = 0$

Otherwise   , then $x(i,j) = 1$

Step-7   Judge the stability of the foundation, considering the design criteria

applicable to the foundation. Let P = 1 in the case of failure and P = 0 in

the case of non-failure.

Step-8   Iterate Steps -3 to -7 a number of times

Step-9   Take the mean of P as the conditional failure probability given γ_i (= $P_{f|\gamma_i}$)

Step-10   Iterate from Step-2 through Step- 9 for all n

Step-11   Calculate the failure probability of the foundation by Equation (5.8) (= P_f)

Step-1 through Step-6 give a spatial distribution of liquefied area given a fraction γ .

We have introduced an indicator random field Z (x, y) in this chapter and we have discussed the spatial distribution of liquefied area and numerical simulation for evaluating the probability of foundation failure using two alternative random models. An application of the numerical simulation to some simple situations are described in the next chapter. Four example cases for evaluating the failure probability in a one-dimensional problem and some examples for simulating the spatial distribution of liquefied area in a two-dimensional problem are given next.
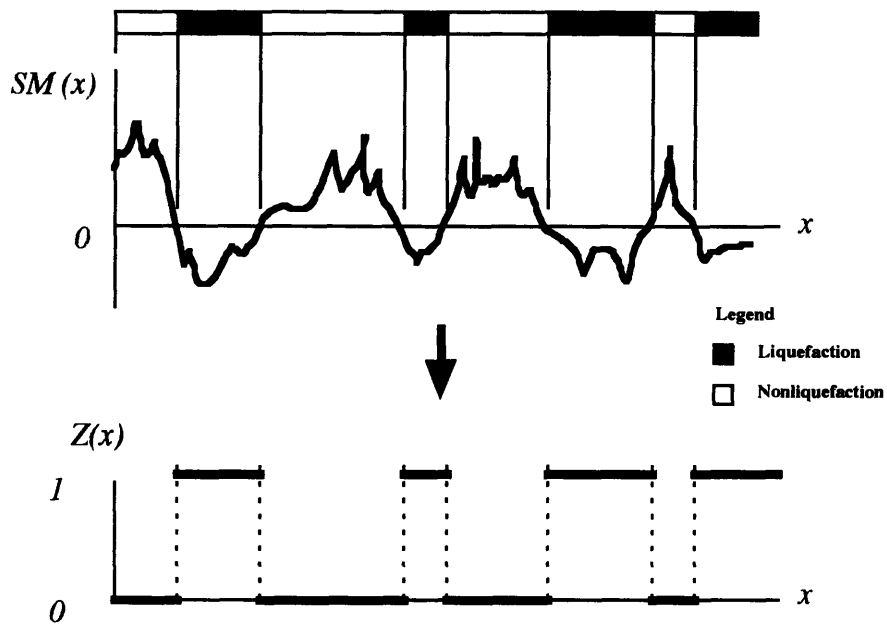
Figure 5.1 Scheme of the Continuous Model in A One-Dimensional Case
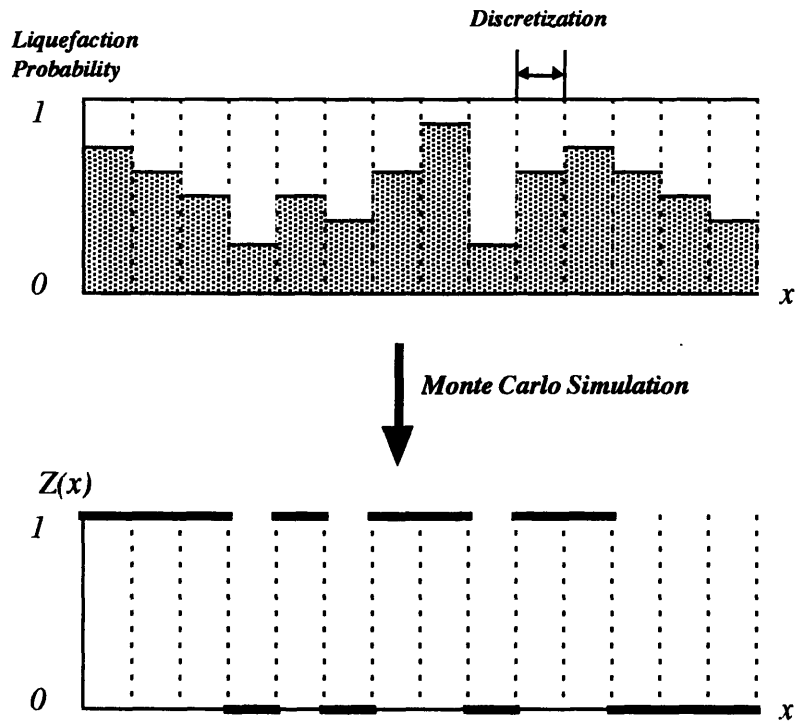

Figure 5.2 Scheme of the Discrete Model in A One-Dimensional Case
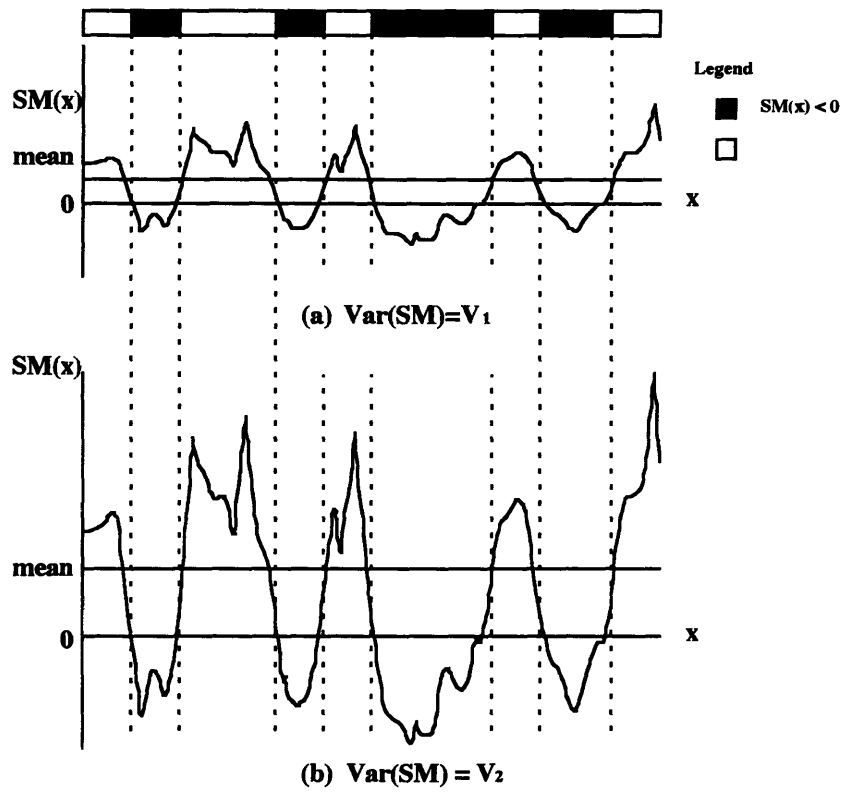
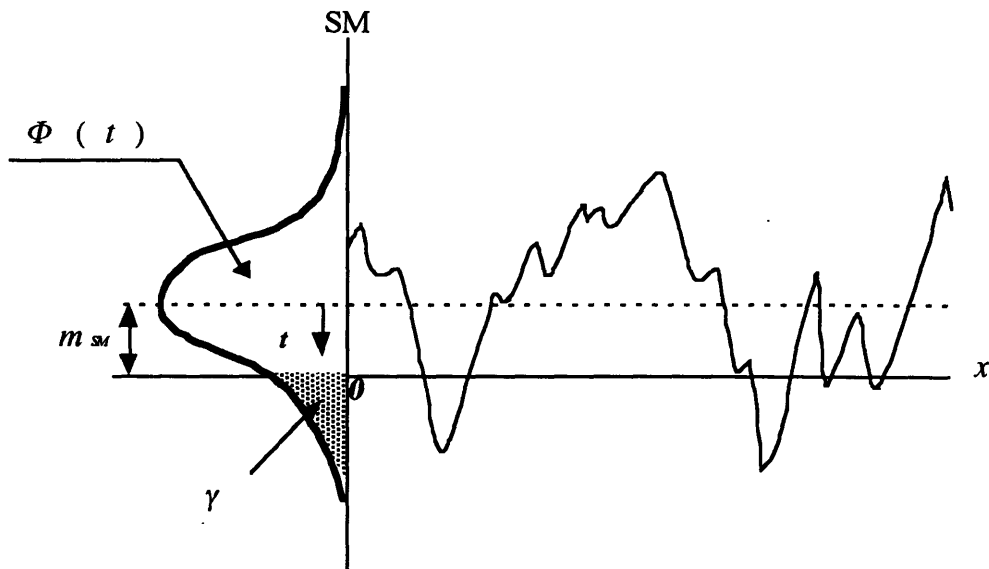Figure 5.3 Zero-Crossing Set and the Magnitude of the Variance

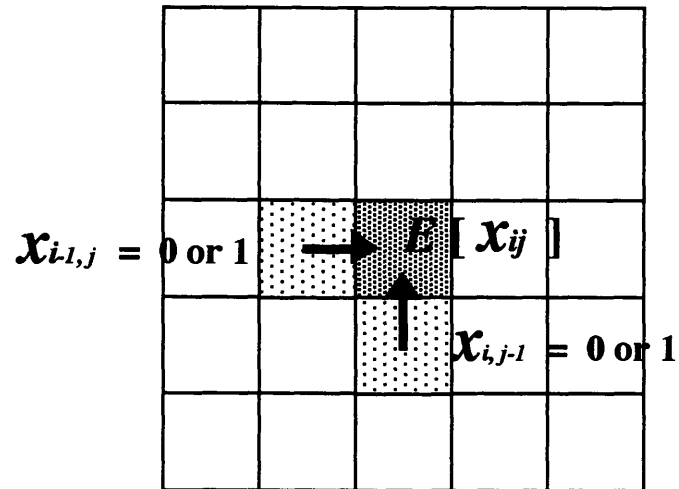Figure 5.4 Relationship between the Mean and the Fraction of Liquefied Area

53

$$X_{i-1,j} = 0 \text{ or } 1 \qquad \xrightarrow{\quad} \quad P\,[\;X_{ij}\;] $$

$$X_{i,j-1} = 0 \text{ or } 1$$

Figure 5.5 Scheme of the Autoregressive Model in A Two-Dimensional Case[6]

---

[6] A simulation result at each grid point represents liquefaction or non-liquefaction in a corresponding square. In this figure, the scheme of the autoregressive model is illustrated in terms of a corresponding square.

CHAPTER VI.   SIMULATION RESULTS

In this chapter, we deal with evaluating the conditional failure probability for a given fraction of liquefied area $P_{f|p}$. This step takes into account the spatial variation of liquefaction and its relation to the behavior of the foundation. Simulation results are presented. Foundations vary in size and shape, and failure criteria depend on the type of structure. Since it is impossible to cover all possible cases, we have focused on a few typical situations. The one-dimensional case is considered first and then some simulation results of the distribution of liquefied area in space are illustrated (that is, only Step-IV mentioned in Chapter III is performed for the two-dimensional cases).

6.1 Four One-Dimensional Cases

We consider two types of foundations, Type-A and Type-B, as mentioned in Chapter III. For each foundation type, we consider two situations :

Type-A foundations

Type-A foundations are continuous as defined in Chapter III. The safety of a continuous foundation depends either on the extent of the liquefied region beneath the foundation, or on the length of the foundation. In general, the larger extent liquefies, the less safe the foundation system becomes for a given foundation. Similarly, the larger the foundation is, the safer the foundation system becomes for a given extent of liquefied region. The following two cases are considered for this type of foundation :

Case-A.1

It is assumed that the foundation fails if a certain fraction of the ground beneath the foundation liquefies. We consider the critical fraction as a parameter, which we vary in different calculations. Figure 6.1 shows the simulation model. The failure probability will be evaluated for critical fractions of liquefied length between 0 and 1.

Case-A.2

In this case, we assume that the fraction of liquefied area necessary to support the superstructure is given. We consider the minimum length (critical length) of the foundation needed to prevent a foundation failure. The critical length of the foundation is treated as a parameter. Figure 6.2 shows the simulation model of Case-A.2. It is assumed in this case that the necessary fraction of liquefied area is 50 percent of foundation length.

<u>Type-B foundations</u>

Type-B foundations consist of several discrete footings. Figure 6.3 shows the simulation model, in which the superstructure is supported by ten equally spaced footings. The stability of the foundation will depend on the number of footings that lose their stability due to soil liquefaction beneath the footings, and on their location. The following two cases are considered for this type of foundation :

Case-B.1

We assume that the stability of the foundation depends only on the total number of the "liquefaction footings"[1]. Stability is independent of the order of the "liquefaction

---

[1] "Liquefaction footings" means the footings such that soil at the center point of each footing liquefies.

footings". It is also assumed that the foundation fails if a certain number of footings turns into "liquefaction footings". We consider the critical number of "liquefaction footings" as a parameter.

Case-B.2

In many practical cases, the order as well as the number of "liquefaction footings" counts for stability of the foundation. In Case-B.2, we assume that the number of the successive "liquefaction footings" determines the foundation stability. The model is otherwise the same as that in Figure 6.3. A parameter that is varied is the maximum number of the successive "liquefaction footings" needed to induce foundation failure.

Simulation Using the Spatially Continuous Model

In this approach, we determine whether or not liquefaction occurs at each point from simulations of the safety margin, as defined in Chapter IV. Figure 6.4 shows example simulations of the safety margin for three different values of the correlation distance ($r_0 = 0.01, 0.1$, and 1.0). In all these cases, the mean safety margin is zero. This figure illustrates the effect of correlation distance. If the mean safety margin is not zero, the plots shift upward or downward by the magnitude of the mean value. Mean values of the safety margin from -1.25 to 1.25 at 0.25 increments are considered below.

Simulation Results

Case-A.1

Simulation results are presented in Figure 6.5 for three values of the ratio between the length of the foundation and the correlation distance (0.1, 1.0 and 10.0). Figure 6.5 (a) corresponds to a high correlation case, whereas Figure 6.5 (c) shows a low correlation

case. The figure illustrates that the mean safety margin and the critical fraction of liquefied length affect the safety of the foundation.

Case-A.2

Simulation results are shown in Figure 6.6. Since it is assumed that the foundation fails when more than half of its length liquefies, the failure probability is 0.5 in the case of zero mean safety margin, regardless of the ratio of the foundation length to the correlation distance. Also, it is concluded that the failure probability is less sensitive to the length of foundation. As the ratio of the foundation length to the correlation distance increases, the failure probability approaches 0, 0.5, or 1.0. These curves will change if a different critical length is selected.

Case-B.1

Figure 6.7 shows simulation results for the following three situations.

Figure 6.7 (a) (Spacing of footings) / r_0 =0.1 and 10 footings

Figure 6.7 (b) (Spacing of footings) / r_0 =1.0 and 10 footings

Figure 6.7 (c) (Spacing of footings) / r_0 =10.0 and 10 footings

In addition, Figure 6.7 (d) shows theoretical results under the condition that the safety margins at the various points are mutually independent. Figure 6.7 (a) corresponds to a high correlation case, whereas Figure 6.7 (c) exhibits a low correlation case. This condition is eventually equivalent to that in Figure 6.7 (d).

Case-B.2

Figures 6.8 shows simulation results for the same three situations as in Case-B.1. A comparison between the two cases (Cases -B.1 and -B.2) indicates that the safety of the

foundation is greatly affected by the criterion of foundation stability. In particular, redundancy in the system improves considerably the level of safety.

Comments on the Simulation Results

Some comments that are common to Case-A and Case-B are made here.

1) *Sensitivity of the failure probability to the critical fraction of liquefied foundation area and the critical number of "liquefaction footings" (effect of the spatial correlation)* : Figures 6.5 (a), 6.7 (a), and 6.8 (a) show that the failure probability of the foundation has a low sensitivity to the fraction of liquefied area (Case-A) and critical number of "liquefaction footings" (Case-B). This fact indicates that, if the spatial correlation in terms of the foundation length and the spacing of footings is large, a change in the critical fraction and the critical number will not affect the safety of the foundation. This is due to the high correlation in the safety margin. Therefore, either the entire foundation experiences liquefaction or the entire foundation is free of liquefaction. As the ratio of the foundation length to the correlation distance (Case-A) and of spacing to correlation distance (Case-B) becomes larger, the failure probability becomes more sensitive to the critical fraction and critical number.

2) *Measures to improve foundation safety* : We can improve the safety of the foundation by increasing the mean safety margin, or by increasing the critical fraction of liquefied area and the critical number of "liquefaction footings". Figures 6.5 through 6.8 illustrate the effects of these measures. For example, comparison between parts (a) and (c) of Figures 6.5, 6.7, and 6.8 suggests that, if the spatial correlation in terms of the length of foundation and the spacing of footings is high, increase in the critical fraction and the critical number will not improve the safety of the foundation. In this case, enhancement of the mean safety margin, by improving soil for instance, will be more

effective. In brief, we can use these figures to choose optimum measures, by considering their cost and effectiveness.

Simulations Using the Spatially Discrete Model

As already discussed in Chapter V for the one-dimensional case, this model is completely specified in terms of the fraction of liquefied area γ and the autoregressive coefficient β. We consider a discretized ground with 100 grid points. The following cases are considered.

Fraction of liquefied area γ = 0.1 to 0.9 at increments of 0.1

Autoregressive coefficient β = 0.1, 0.5 and 0.9

Simulation results for the failure probability are shown in Figures 6.9 (Case-A.1), Figure 6.10 (Case-A.2), Figures 6.11 (Case-B.1), Figure 6.12 (Case-B.2).

A small failure probability corresponds to a large mean safety margin in the spatially continuous model. Also, a small autoregressive coefficient corresponds to a small correlation distance. For example, the plots in Figure 6.11 (a) (Case-B.1, β = 0.1) agree with theoretical results in Figure 6.7 (d) where the safety margins at various points are mutually independent.

Comments on the Simulation Results

The conclusions drawn from these simulation results are similar to those for the spatially continuous model. We, therefore, focus on the difference between the two models.

Ease of computation : In general, the spatially discrete model is much superior to the

spatially discrete model in terms of computation time[2] and simplicity of the computer code. If the autoregressive coefficients can be determined from given field observation data, the use of the spatially discrete model is recommended.

6.2 Two-Dimensional Cases

The two probabilistic models of spatial liquefaction are applied here to two-dimensional problems. We consider a one-by-one square region which consists of 51 x51 simulation points. We focus on two points : (1) effect of the spatial correlation and (2) effect of anisotropy. Example simulations of liquefied patterns in the following cases are shown.

Simulation Using the Spatially Continuous Model

Four different values of correlation distance shown below are selected in Case-1. It is assumed that the mean safety margin is zero.

Case-1 Correlation distance r_0 = 0.01, 0.1, 0.3, and 0.6

     (for simulation results of liquefied patterns, see Figures 6.13 (a)

     through 6.13 (d))

Simulation Using the Spatially Discrete Model

In Cases -2 and -3, we deal with an isotropic field (β_1 = β_2). Two different values of the fraction of liquefied area (γ = 0.1 and 0.5) are considered and then two different set of autoregressive coefficients (β_1 = β_2 = 0.1 and 0.9) are selected for each value of the fraction. The value of the fraction γ = 0.1 represents a low correlated case, whereas γ = 0.9 stands for a highly correlated case.

---

[2] Generation of $\hat{X}(t)$ using Equations (A.42) and (A.43) requires a number of iteration.

Case-2 $\gamma = 0.1$, $\beta_1 = \beta_2 = 0.1$, and 0.9 (see Figure 6.14, (a) and (b))

Case-3 $\gamma = 0.5$, $\beta_1 = \beta_2 = 0.1$, and 0.9 (see Figure 6.15,.(a) and (b))

In order to consider an anisotropic field, we choose different values for β_1 and β_2. A set of autoregressive coefficients (β_1 , β_2) = (0.9, 0.1) models a vertically highly correlated and horizontally low correlated case. A reverse situation is given by (β_1 , β_2) = (0.1, 0.9). Two different values of the fraction γ for these two situations are also considered.

Case-4 $\gamma = 0.1$,   (β_1 , β_2) = (0.9, 0.1), and (0.1, 0.9)

(see Figure 6.16, (a) and (b).)

Case-5 $\gamma = 0.5$,   (β_1 , β_2) = (0.9, 0.1), and (0.1, 0.9)

(see Figure 6.17, (a) and (b).)

From Figures 6.13, 6.14 and 6.15, we can see that the liquefied regions tend to flock together as the correlation distance (equivalent to the autoregressive coefficients) increases. Also, Figures 6.16 and 6.17 show the effect of anisotropy explicitly. Liquefied regions tend to form longitudinally in Figures 6.16 (a) and 6.17 (a), whereas Figures 6.16 (b) and 6.17 (b) exhibit a horizontal succession of liquefaction/non-liquefaction regions. It is obvious that the fraction of liquefied area affects the number of liquefaction points in Figures 6.14 through 6.17. That is, the larger the value of the fraction is, the more liquefaction points we have. The fraction of liquefied area corresponds to the mean safety margin in Case-1 (Figure 6.13).

1.0

e.g. An Oil Tank

a   b   c   d   e

Legend

■ **Non-liquefied area**

□ **Liquefied area**
   (by a simulation)

Fraction of Liquefied Area

= **Length of (a+b+c+ . . .) / 1.0**
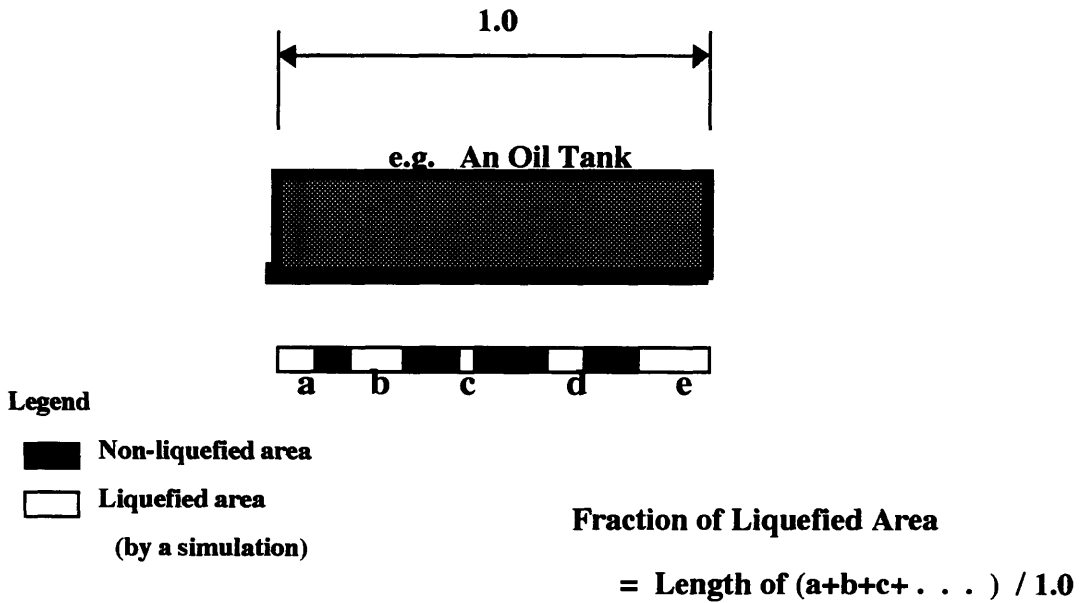
Figure 6.1 Simulation Model for Case-A.1

Model Ground L=1.0

A Foundation

A Variable

•
•
•
•
•

(Assumption)
The foundation fails
when more than half
of the foundation area
liquefies.
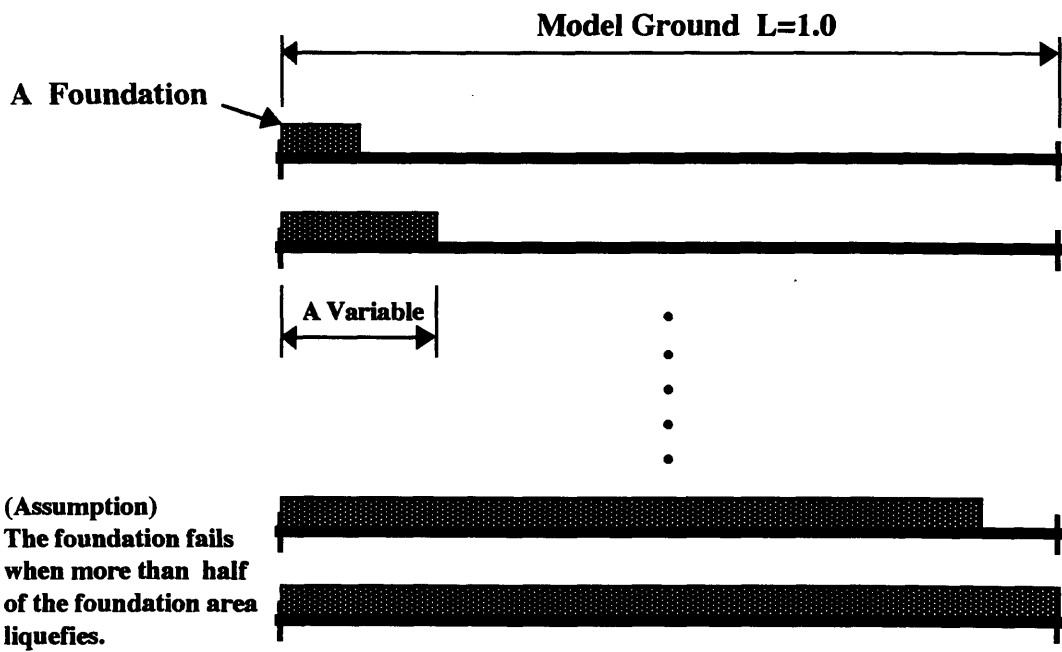
Figure 6.2 Simulation Model for Case-A.2

63

Superstructure supported by ten equally spaced footings

A footing

Ground Surface

(Assumption)
The stability of each
foundation is determined
by the occurrence of the
liquefaction at each
simulation point below the
footing.

Points of the
simulation trial

The result of simulation trials at this
point will determine the stability of
the foundation on it.
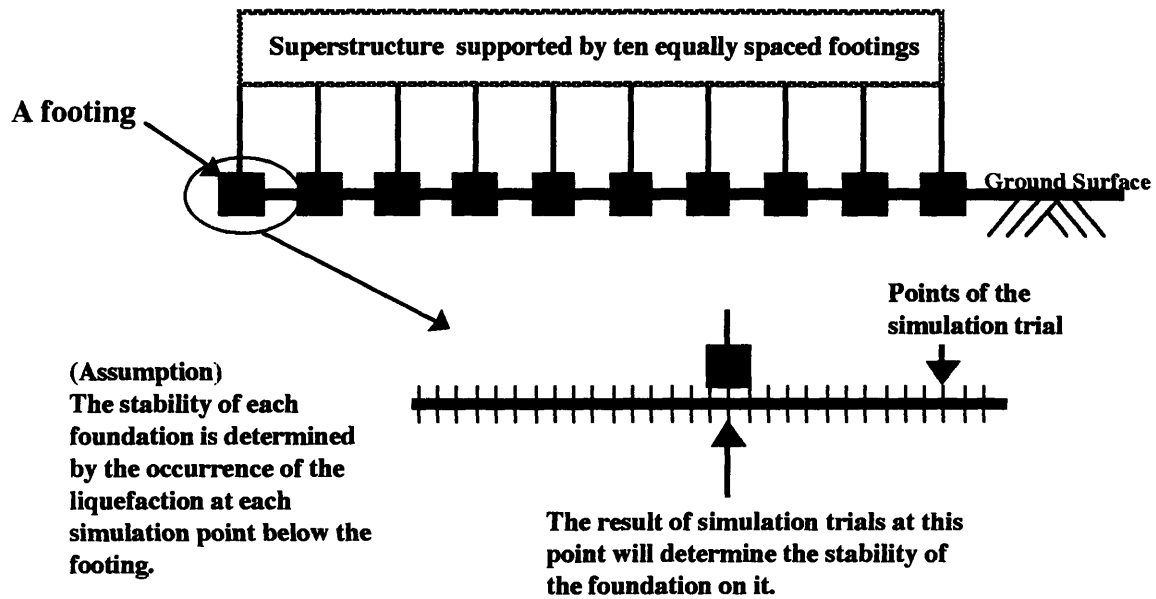
Figure 6.3 Simulation Model for Case-B.1 and Case-B.2
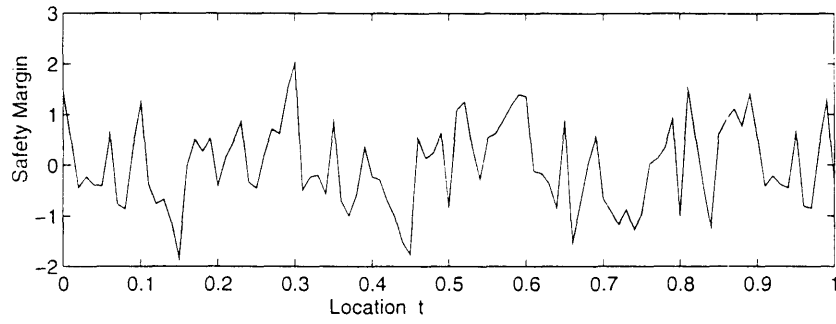
(a) $r_0 = 0.01$
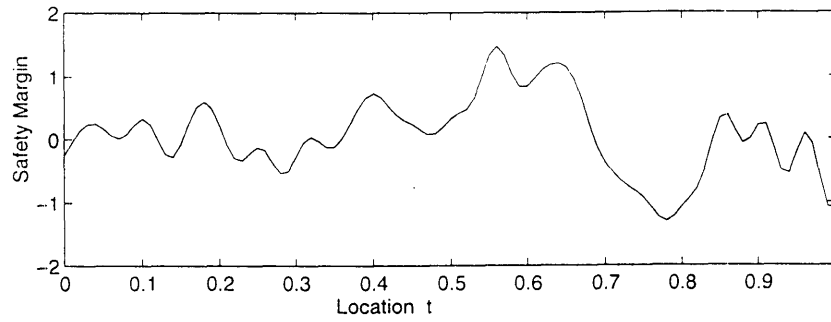
(b) $r_0 = 0.1$
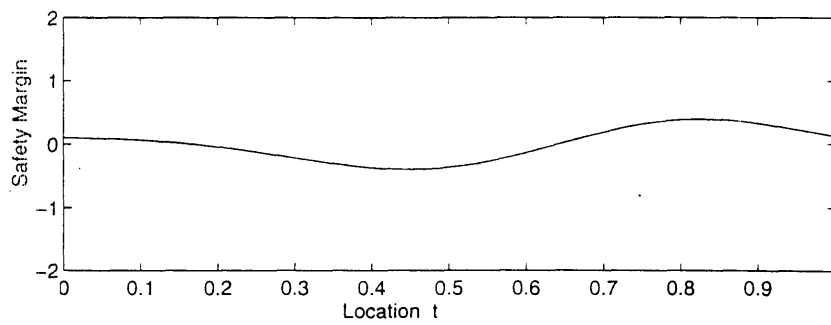
(c) $r_0 = 1.0$

Figure 6.4   Simulation Results of the Safety Margin
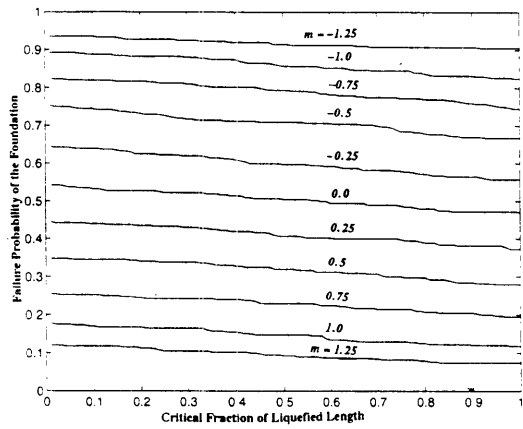
Figure 6.5 (a)   Case-A.1 :
$$L_{foundation} / r_0 = 0.1$$
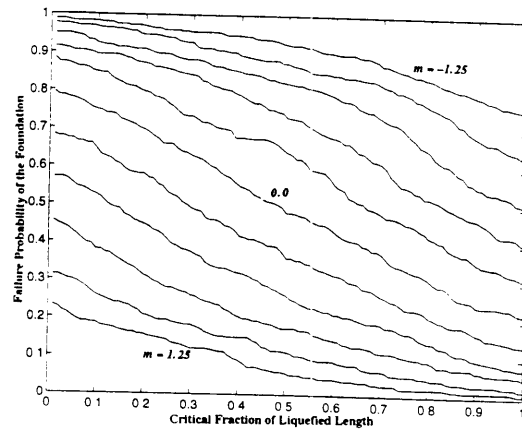
Figure 6.5 (b)   Case-A.1 :
$$L_{foundation} / r_0 = 1.0$$
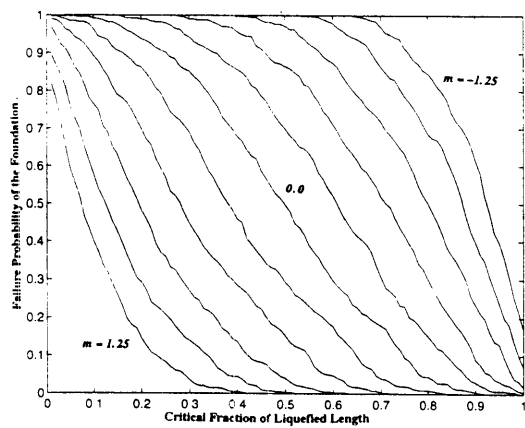
Figure 6.5 (c)   Case-A.1 :
$$L_{foundation} / r_0 = 10.0$$

Figure 6.6 Case-A.2

66
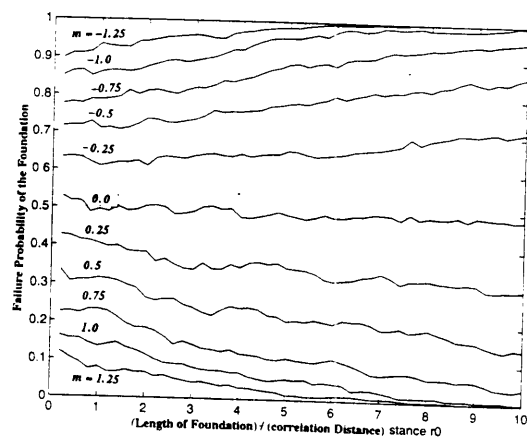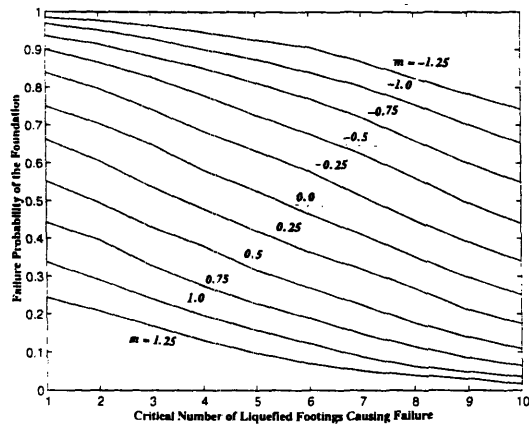
Figure 6.7 (a)   Case-B.1 :

Spacing / r₀ = 0.1   and   10   footings
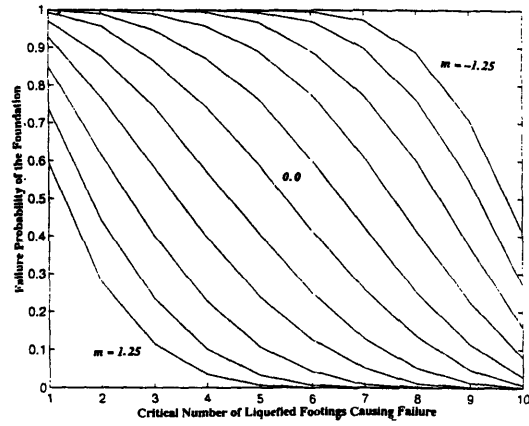
Figure 6.7 (b)   Case-B.1 :

Spacing / r₀ = 1.0   and   10   footings
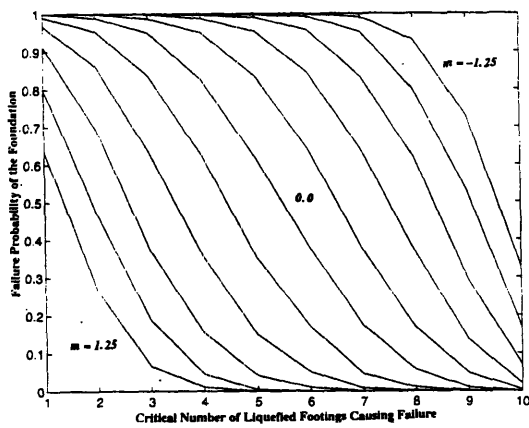
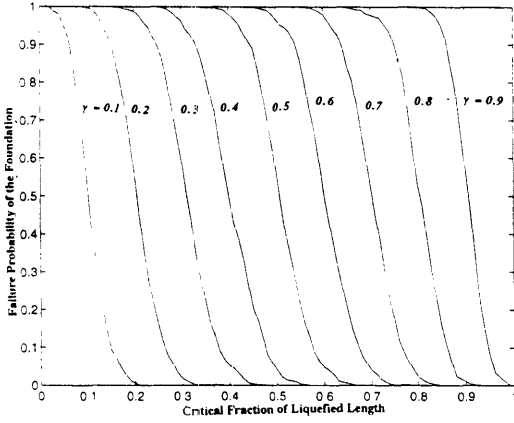Figure 6.7 (c)   Case-B.1 :

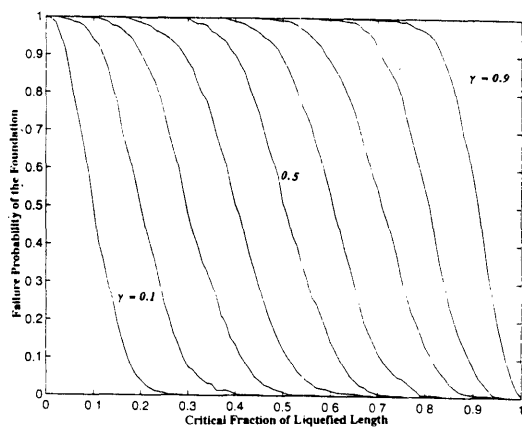*Spacing / r₀ = 10.0   and   10   footings*
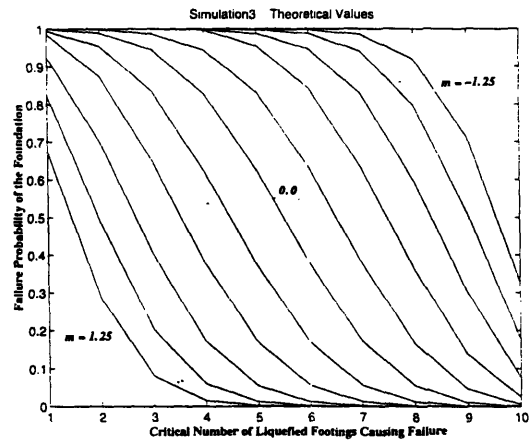
Figure 6.7 (d)   Case-B.1 :

Theoretical Values
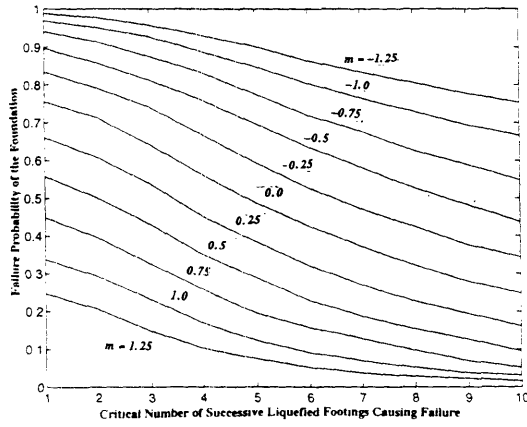
Figure 6.8 (a)   Case-B.2 :

Spacing / r_0 = 0.1   and   10   footings
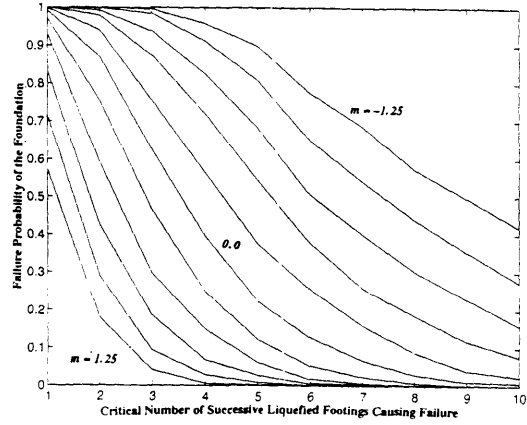
Figure 6.8 (b)   Case-B.2 :

Spacing / r_0 = 1.0   and   10   footings
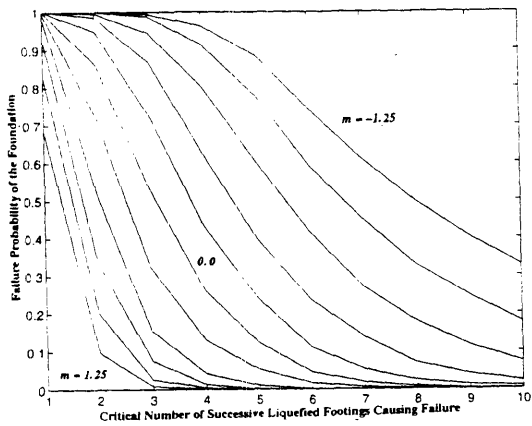
Figure 6.8 (c)   Case-B.2 :

Spacing / r_0 = 10.0   and   10   footings

Figure 6.9 (a)   Case-A.1 : β = 0.1
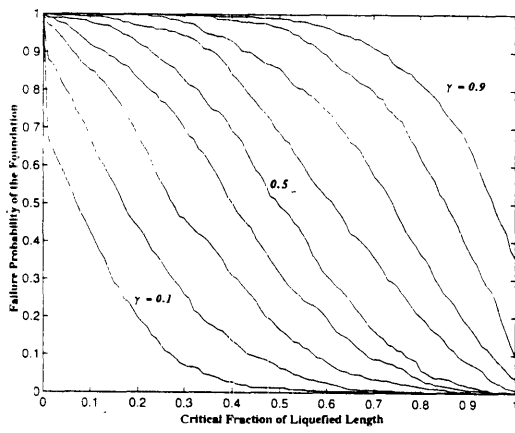

Figure 6.9 (b)   Case-A.1 : β = 0.5

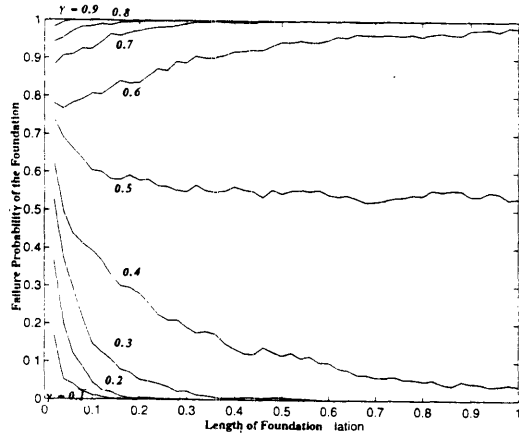Figure 6.9 (c)   Case-A.1 : β = 0.9
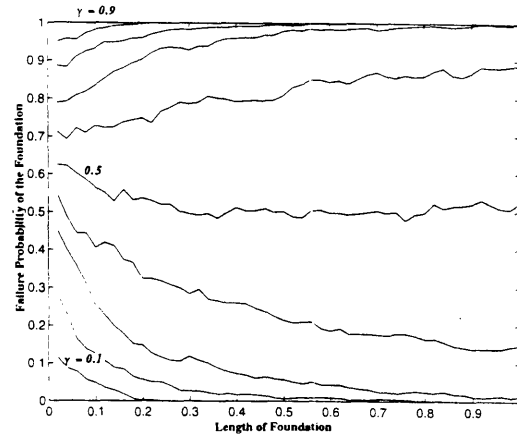
Figure 6.10 (a)   Case-A.2 : β = 0.1

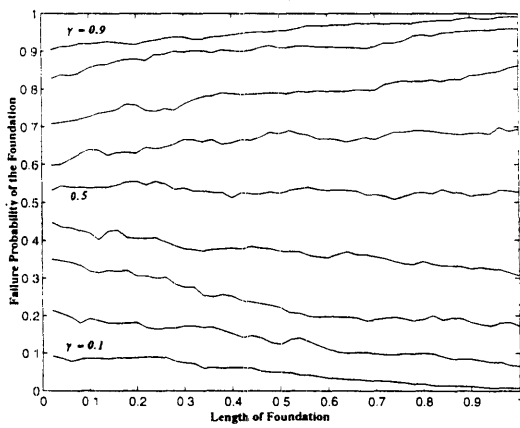Figure 6.10 (b)   Case-A.2 : β = 0.5

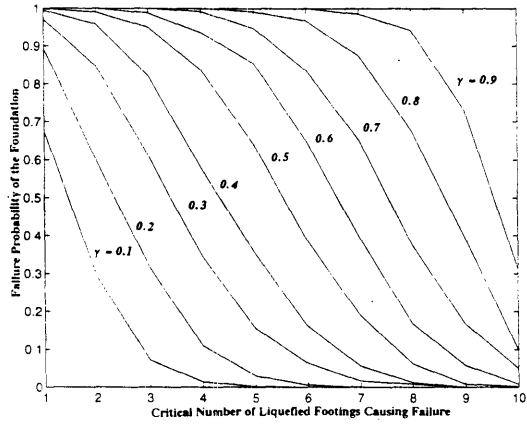Figure 6.10 (c)   Case- A.2 : β = 0.9

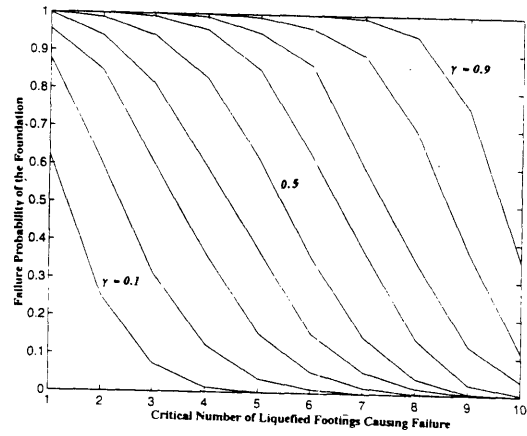Figure 6.11 (a)   Case-B.1: $\beta = 0.1$

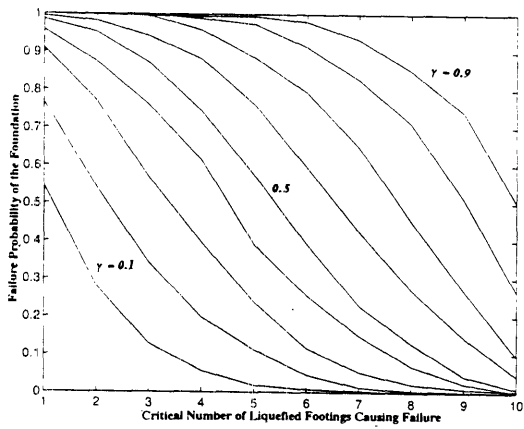Figure 6.11 (b)   Case-B.1 : $\beta = 0.5$
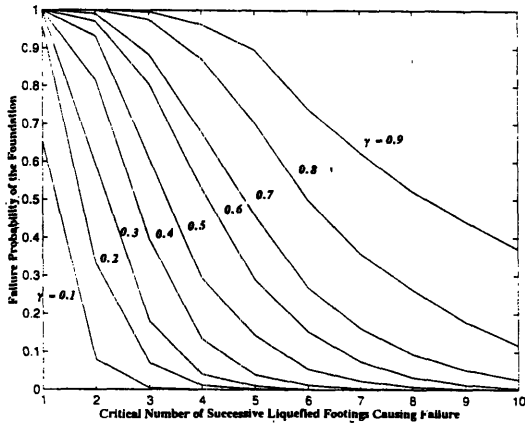

Figure 6.11 (c)   Case-B.1 : $\beta = 0.9$

71

Figure 6.12 (a)   Case- B.2 : β = 0.1
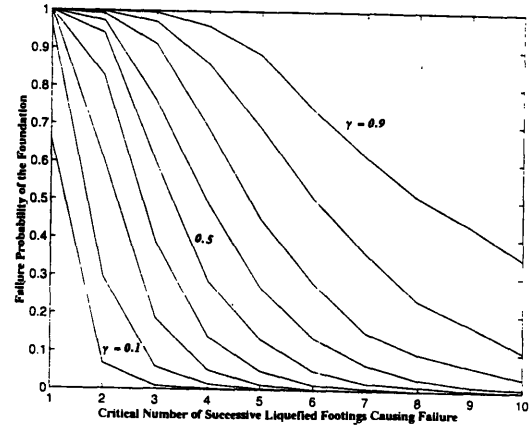
Figure 6.12 (b)   Case-B.2 : β = 0.5
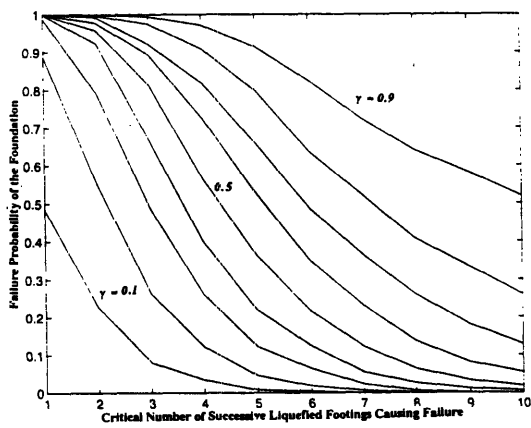
Figure 6.12 (c)   Case-B.2 : β = 0.9
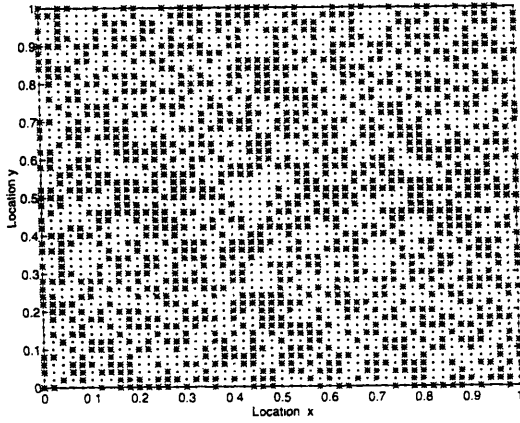
Figure 6.13 (a)   Case-1 : r_0 = 0.01
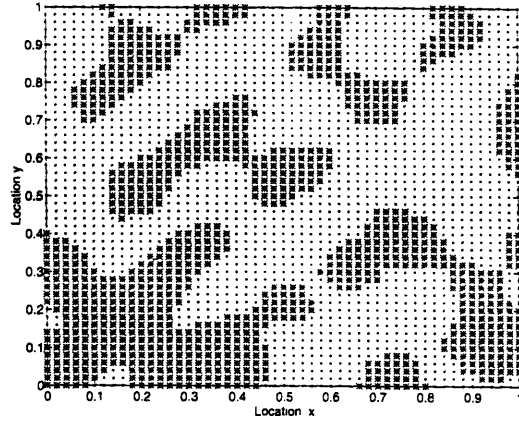
Figure 6.13 (b)   Case-1 : r_0 = 0.1
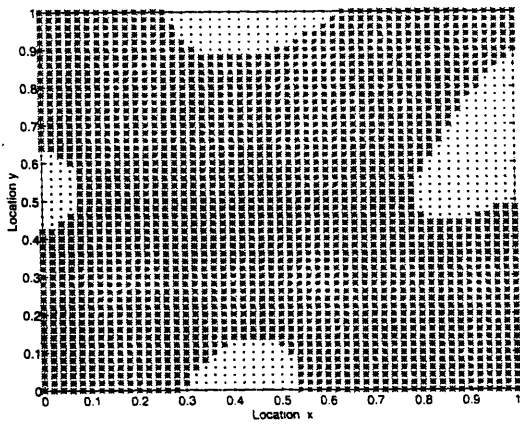
Figure 6.13 (c)   Case-1 : r_0 = 0.3
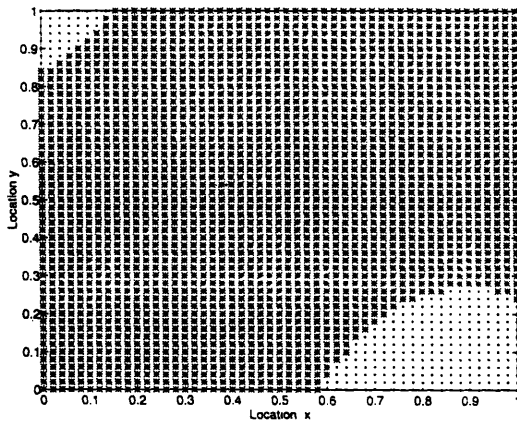
Figure 6.13 (d)   Case-1 : r_0 = 0.6
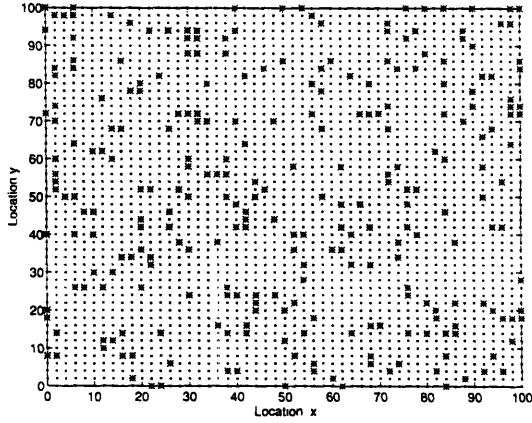
Figure 6.14 (a)   Case-2 :

$\gamma = 0.1, \quad \beta_1 = \beta_2 = 0.1$
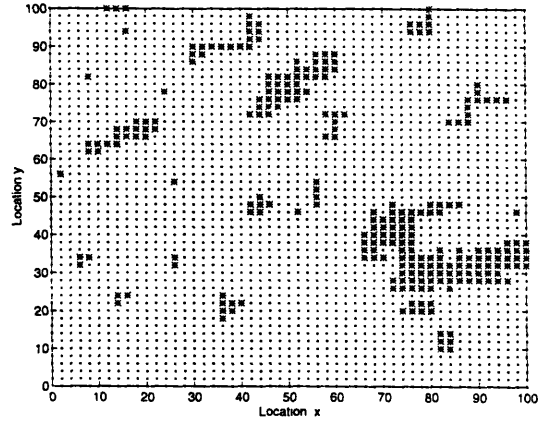
Figure 6.14 (b)   Case-2 :

$\gamma = 0.1, \quad \beta_1 = \beta_2 = 0.9$
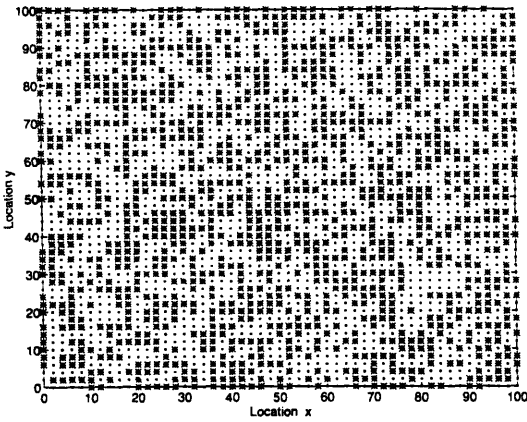
Figure 6.15 (a)   Case-3 :

$\gamma = 0.5, \quad \beta_1 = \beta_2 = 0.1$
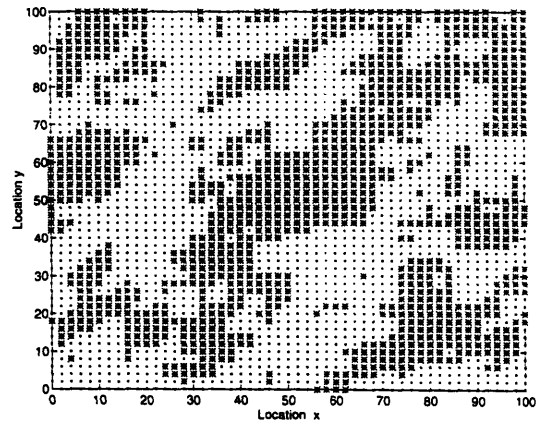
Figure 6.15 (b)   Case-3 :

$\gamma = 0.5, \quad \beta_1 = \beta_2 = 0.9$
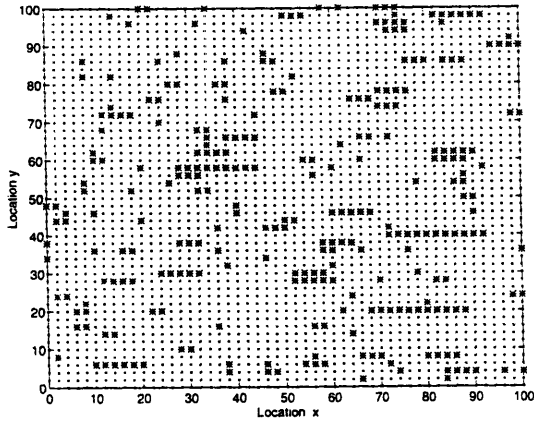
Figure 6.16 (a)   Case-4 :

$\gamma = 0.1$, $\beta_1 = 0.9$ $\beta_2 = 0.1$
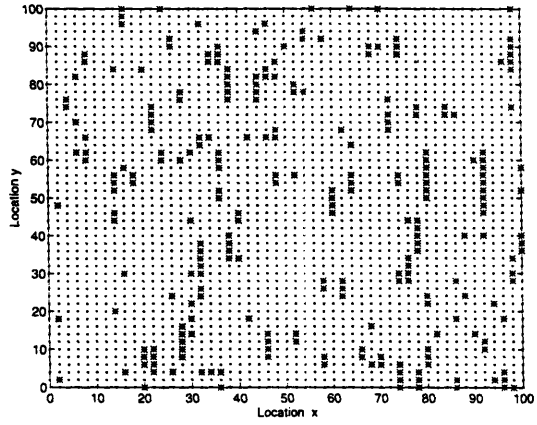
Figure 6.16 (b)   Case-4 :

$\gamma = 0.1$, $\beta_1 = 0.1$ $\beta_2 = 0.9$
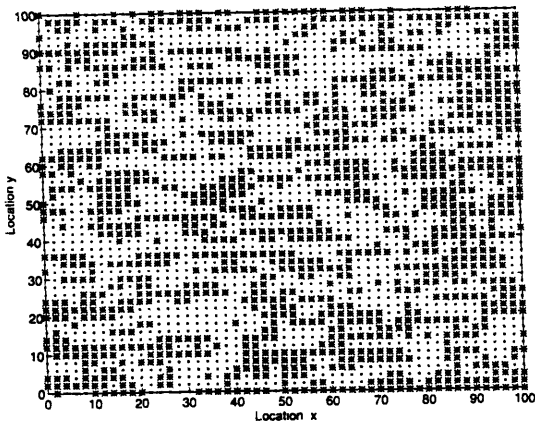
Figure 6.17 (a)   Case-5 :

$\gamma = 0.5$, $\beta_1 = 0.9$ $\beta_2 = 0.1$
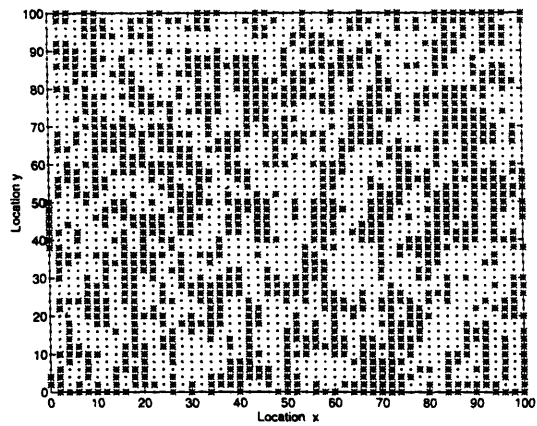
Figure 6.17 (b)   Case-5 :

$\gamma = 0.5$, $\beta_1 = 0.1$ $\beta_2 = 0.9$

CHAPTER VII.   CONCLUSIONS

A methodology for evaluating the safety of spatially extended foundations against liquefaction has been presented. The objective is to extend the usual analysis of liquefaction risk at a point to account for the spatial variability of the phenomenon and for the failure criterion of the system at risk.

First, the uncertainty in the fraction of liquefied area, γ , was examined. For a given region, the fraction γ varies not only with M and R but also from earthquake to earthquake. In addition, the fraction γ varies from site to site for a given earthquake. It is important to quantify this variability; however, we can only resort to engineering judgment at this stage. Spatial variability is also crucial to the evaluation of safety. To describe the spatial pattern of liquefaction, we assigned a binary value, either 1 (liquefaction) or 0 (non-liquefaction), as a spatial correlated binary function. Two random field models are used : (1) the spatially continuous model (Model-1) and (2) the spatially discrete model (Model-2). Spatial dependence of liquefaction was taken into account in the form of correlation distance in Model-1 and autoregressive coefficients in Model-2. Since foundations vary in size and shape, and failure criteria depend on the type of structure, no analytical method can cover all possible situations. Therefore, we here illustrated the evaluation of safety for a few foundation systems through numerical simulation. The probability of foundation failure is obtained by taking the integral of the product of the conditional failure probability for a given fraction γ and the probability density function of the fraction γ .

Applying the proposed methodology to several simple one and two-dimensional problems, some numerical experiments were performed and the safety of the foundations was expressed in terms of the failure probability. The sensitivity of the failure probability

to the critical fraction of liquefied area and the critical number of "liquefaction footing" was examined based on the results. If the spatial correlation is large, the failure probability is less sensitive to the two parameters, namely, the critical fraction of liquefied area and critical number of "liquefaction footings". Also, these simulation results can give information about the measures to improve the foundation safety. In general, a simulation based on Model-2 requires much less time than that based on Model-1. If the autoregressive coefficients can be determined from given field observation data, the use of Model-2 is recommended.

A few future extensions and refinements of the proposed methodology are desirable. These include :

1) Variability of the Fraction of Liquefied Area : As mentioned in Chapter IV (Section 4.4), the fraction of liquefied area has some variability. This is important because it affects the evaluation of foundation safety. However, since no research is available at present, future work is essential. This variability may be seen by analyzing past liquefaction records. We suggest that data concerning the liquefied area be collected.

2) Propagation of the Liquefied Region : The propagation of the liquefied region should be taken into account. However, the phenomenon is so complicated that its mechanism is not fully understood. It would be acceptable to consider that the propagation of liquefaction easily happens when a soil deposit has a small liquefaction resistance. In such a situation, we may adjust the magnitude of spatial correlation to some extent (in this particular case, use a larger value of spatial correlation than originally estimated) in order to take into account the propagation effect.

3) <u>Non-Homogeneous Grounds</u> : Since we often encounter non-homogeneous grounds in actual engineering situations, dealing with them is important (non-homogeneity means that the fraction of liquefied area depends on location). We can simulate the spatial pattern of liquefaction in a non-homogeneous ground by varying the fraction of liquefied area (the mean safety margin) in the spatially continuous model or the autoregressive coefficients in the spatially discrete model according to its non-homogeneity.

4) <u>Three-Dimensional Problems (Type-C Foundations in Chapter III)</u> : In this research, only horizontal problems have been considered. As discussed in Chapter III, the vertical problems also need to be dealt with. This problem can be handled by applying the proposed methodology to a vertical direction as well as a horizontal direction.

APPENDIX   CORRELATION THEORY OF RANDOM FIELDS

The theoretical background of the correlation theory of random fields is briefly described. Yaglom (1963), Veneziano (1978), and Vanmarcke (1983) present its theory in a much deeper and broader context.

Definition and Complete Representation of A Random Field

Consider a real valued function x (ω, $\underline{t}$)   where $\underline{t}$ belongs to R^n, the n-dimensional space, and ω belongs to the set Ω of the possible outcomes of a random experiment. The values of the function are random numbers due to their dependence on ω. Therefore, this function is called a random field in R^n (in particular, a random process in R^1). We are usually interested either in the deterministic field resulting from fixing ω, or in the random variable resulting from fixing $\underline{t}$. Hereinafter, the former is denoted by $x(\underline{t})$ and the latter is denoted by $X(\underline{t})$.

A random field is considered to be completely specified if we are given the cumulative distribution function :

$$F_{\underline{t}}\ (x)\ =\ P\ [\ X\ (\underline{t})\ <\ x\ ] \tag{A.1}$$

of the random variable $X(\underline{t})$ for each $\underline{t}$ in R^n, and in general if we are given the joint cumulative distribution function :

$$F_{\underline{t}_1,\ \cdots,\underline{t}_k}(\ x_1,\ \cdots,\ x_k)\ =\ P\ [\ X(\underline{t}_1)\ <\ x_1,\ \cdots,\ X(\underline{t}_k)\ <\ x_k\ ] \tag{A.2}$$

of $X(\underline{t}_1)$, $\cdots$, $X(\underline{t}_k)$ for any k points $\underline{t}_1$, $\cdot\ \cdot\ \cdot$, $\underline{t}_k$ in R^n.

Homogeneity and Isotropy

A random field is said to be homogeneous if all its cumulative distribution functions are invariant with respect to identical translation (not rotation) of the parameters $t_1, \cdots, t_k$, in other words, if all the distribution functions depend only on the relative location of the points and not on absolute location. Incidentally, the term "stationary" instead of the term "homogeneous" is used for a random process, i.e. a one-dimensional random field. As for isotropy, a random field is said to be isotropic if all its cumulative distribution functions are invariant with respect to rigid-body motions, including translation and rotation, and with respect to mirror reflections.

Mean Value and Autocovariance Function

In most practical situations, few properties of the random fields dealt with are known to us. Instead, all we know (or assume) are the mean and covariance function of the random field.

Mean:
$$m(\underline{t}) = E[X(\underline{t})] \tag{A.3}$$

Covariance:

$$B(\underline{t}_1, \underline{t}_2) = E[(X(\underline{t}_1) - m(\underline{t}_1))(X(\underline{t}_2) - m(\underline{t}_2))] \tag{A.4}$$

$$= E[X(\underline{t}_1) X(\underline{t}_2)] - m(\underline{t}_1) m(\underline{t}_2)$$

$B(\underline{t}_1, \underline{t}_2)$ is called the autocovariance function of $X(\underline{t})$. The theory of random fields that make use only of the mean value function and of the autocovariance function is called correlation theory. The normalized autocovariance function :

$$\rho(\underline{t}_1, \underline{t}_2) = B(\underline{t}_1, \underline{t}_2) / \sigma(\underline{t}_1) \sigma(\underline{t}_2), \tag{A.5}$$

is called the autocorrelation function of $X(\underline{t})$. Hence, $\rho(\underline{t}_1, \underline{t}_2)$ is the correlation

coefficient between $X(\underline{t}_1)$ and $X(\underline{t}_2)$ and is bounded between -1 and 1. When we deal with homogeneous fields, we can write m instead of $m(\underline{t})$, i.e. the mean value is constant, and $B(\underline{\tau})$ instead of $B(\underline{t}_1,\underline{t}_2)$, i.e. the autocovariance depends only on the vector:

$$\underline{\tau} \; = \; \underline{t}_2 - \underline{t}_1 \tag{A.6}$$

and not on the location of the points $\underline{t}_1$ and $\underline{t}_2$. For isotropic fields, the covariance depends only on the distance between the two points.

$$r \; = \; |\underline{\tau}| \; = \; |\underline{t}_2 - \underline{t}_1| \tag{A.7}$$

The following autocovariance functions are widely used for isotropic random fields. These covariance functions are valid in one, two, and three-dimensions. See Figure A.1.

1) Simple exponential

$$B(r) \; = \; \sigma^2 e^{-r/r_0} \tag{A.8}$$

where r_0 : correlation distance

This is a proper autocovariance function in spaces of any dimension; it has been frequently used to model spatial variation of soil properties.

2) Exponentially damped cosine function

$$B(r) \; = \; \sigma^2 e^{-r/r_0} \cos \beta r, \quad r_0 < \sqrt{3} \, / \, 3\beta \tag{A.9}$$

3) Double exponential

$$B(r) \; = \; \sigma^2 e^{-(r/r_0)^2} \tag{A.10}$$

Gaussian Random Fields

The mean and autocovariance functions are not sufficient information to completely specify a random field. However, if the field is Gaussian, these two functions are enough information for the complete specification.

Ergodicity

We define the operator $< \ >$ as shown below[1] :

$$< \ f(\underline{t}) \ > \ = \ \lim_{D^n \to R^n} \frac{1}{D^n} \int_{D^n} f(\underline{t}) d\underline{t} \qquad (A.11)$$

where D^n is a subset of the space R^n, i.e. its length, area, or volume whichever is appropriate, and $f(\underline{t})$ is a function. This operator produces spatial averages, whereas, by comparison, the operator E produces statistical averages across the ensemble (expectations). A homogeneous random field is called ergotic if these two operators produce the same results. Note that although ergodicity in some property implies homogeneity in that same property, the reverse is not necessarily true. For an ergotic random field, we will have :

$$m \ = \ < \ x(\underline{t}) \ > \qquad (A.12)$$

$$B(\underline{\tau}) \ = \ < \ (x(\underline{t}) - m) \ (x(\underline{t} + \underline{\tau}) - m) \ > \qquad (A.13)$$

for any realization $x(\underline{t})$ of the random field $X(\underline{t})$. In most cases, random fields occurring in practice are assumed to be ergotic.

---

[1] The symbol $\int_{D^n}$ is used instead of $\underbrace{\int \cdots \int}_{n \ times}$ and the symbol $d\underline{t}$ is used instead of $dt_1 \cdots dt_n$.

Also, D_n stands for both the region and its measure.

Spectral Representation of Random Fields

Let $X(\underline{t})$ be a homogeneous Gaussian random field with mean zero. $X(\underline{t})$ may be represented as the real part of a complex random field $X^*(\underline{t})$:

$$X(\underline{t}) = \text{Re}\left\{ X^*(\underline{t}) \right\} = \text{Re}\left\{ \int_{R^n} e^{i\underline{\omega}^T \underline{t}} Z(d\underline{\omega}) \right\} \tag{A.14}$$

where $\underline{\omega}^T \cdot \underline{t}$ denotes the dot product of the two vectors $\underline{\omega}$ and $\underline{t}$, and $Z(d\underline{\omega})$ is an uncorrelated random function with the following properties.

1) For all intervals $\Delta\underline{\omega}$,

$$E\ [Z(\Delta\underline{\omega})] = 0. \tag{A.15}$$

2) For any disjoint intervals $\Delta_1\underline{\omega}$ and $\Delta_2\underline{\omega}$,

$$Z\ (\Delta_1\underline{\omega} + \Delta_2\underline{\omega}) = Z\ (\Delta_1\underline{\omega}) + Z\ (\Delta_2\underline{\omega}) \tag{A.16}$$

and

$$E\ [\ Z(\Delta_1\underline{\omega})\ Z(\Delta_2\underline{\omega})\ ] = 0 \tag{A.17}$$

Equation (A.14) expresses $X^*(\underline{t})$ as the sum of many uncorrelated component functions of the form $e^{i\omega t} = \cos\omega t + i\sin\omega t$, each associated with a small interval $d\omega$ on the frequency axis and each multiplied by a complex random amplitude $Z(d\underline{\omega})$ with mean zero. Thus, we may write $X(\underline{t})$ as :

$$X(\underline{t}) = \int_{R^n}\cos(\ \underline{\omega}^T \cdot \underline{t}\ )\ Z(d\underline{\omega})\ . \tag{A.18}$$

The variance of $X(\underline{t})$ is :

$$Var\ [\ X(\underline{t})\ ] = \int_{R^n} E[\ |\ Z(d\underline{\omega})\ |^2\ ] = \int_{R^n} S(\underline{\omega})\ d\underline{\omega}. \tag{A.19}$$

The function $S(\underline{\omega})$ is called the two-sided spectral density function of the random field. In order to evaluate the covariance function of $X(\underline{t})$, we insert $X(0)$ and $X(\tau)$ into the definition, and interchange the operations of integration and expectation. Then, we obtain :

$$
\begin{aligned}
B(\tau) = Cov\ [\ X(0),\ X(\tau)\ ] &= E\left[\ \int_{R^n} Z(d\underline{\omega})\ \int_{R^n}\cos(\underline{\omega}^T \cdot \underline{t})\ Z(d\underline{\omega})\ \right] \\
&= \int_{R^n} \cos(\underline{\omega}^T \cdot \underline{t})\ E\left[\ |\ Z(d\underline{\omega})\ |^2\ \right]
\end{aligned}
\tag{A.20}
$$

Combining the equations (A.19) and (A.20) generates the Wiener-Khinchine relations :

$$
B(\underline{\tau}) = \int_{R^n} \cos(\underline{\omega}^T \cdot \underline{\tau})\ S(\underline{\omega})\ d\underline{\omega}
\tag{A.21}
$$

and

$$
S(\underline{\omega}) = \frac{1}{(2\pi)^n} \int_{R^n} \cos(\underline{\omega}^T \cdot \underline{\tau})\ B(\underline{\tau})\ d\underline{\tau}.
\tag{A.22}
$$

Since $B(\underline{\tau}) = B(-\underline{\tau})$, the function $S(\underline{\omega})$ is symmetric about $\underline{\omega} = \underline{0}$. There is only one function satisfying equations (A.21) and (A.22) for each function $B(-\underline{\tau})$. For isotropic fields, $S(\underline{\omega})$ depends only on $\omega = |\ \underline{\omega}\ |$. Thus, we can write $S(\omega)$ instead of $S(\underline{\omega})$. We can interpret $X(\underline{t})$ as the result of superimposing, to its mean value, many functions of the form $\cos(\underline{\omega}^T \cdot \underline{t})$, each of which has a different $\underline{\omega}$,and each of which is multiplied by a random amplitude $Z(d\underline{\omega})$ with zero mean and variance $S(\underline{\omega})d\underline{\omega}$.

As an example, if the correlation function has the exponential form, $\rho(r) = e^{-r/r_0}$, then the spectral density functions in R^1, R^2, and R^3 are as follows :

$$
S_1(\omega) = \frac{r_0}{\pi(1 + \omega^2 r_0^2)} \qquad \text{for } R^1 \tag{A.23}
$$

84

$$S_2(\omega) = \frac{\alpha}{2\pi(\alpha^2 + \omega^2)^{3/2}} \;,\quad \alpha = \frac{1}{r_0} \qquad \text{for } R^2 \qquad \text{(A.24)}$$

$$S_3(\omega) = \frac{r_0^3}{\pi^2(1 + \omega^2 r_0^2)^2} \qquad\qquad \text{for } R^3 \qquad \text{(A.25)}$$

Figure A.2 illustrates the spectral density functions $S_1(\omega)$ and $S_2(\omega)$.

Simulation of Homogeneous Gaussian Random Fields

Again, let $X(\underline{t})$ be a n-dimensional homogeneous Gaussian random field with zero mean, covariance function $B(\underline{\tau})$ and spectral density function $S(\underline{\omega})$. According to (A.18), $X(\underline{t})$ is :

$$X(\underline{t}) = \int_{R^n} \cos(\underline{\omega}^T \cdot \underline{t}) \; Z(d\underline{\omega}). \qquad\qquad \text{(A.26)}$$

A homogeneous random field $X(\underline{t})$ with mean zero can be expressed as a sum of sinusoids with random amplitudes $C(d\underline{\omega})$ and phase angles $\phi(\underline{\omega})$.

$$X(\underline{t}) = \int_{R^n} C(d\underline{\omega}) \cos(\underline{\omega}^T \cdot \underline{t} + \phi(\underline{\omega})) \qquad\qquad \text{(A.27)}$$

The variance of $X(\underline{t})$ is :

$$[\ X(\underline{t})\ ] = \int_{R^n} E\ [\ X^2(\underline{t})\ ] = \int_{R^n} E[\ C^2(d\underline{\omega})\ ]\ E[\ \cos^2(\underline{\omega}^T \cdot \underline{t} + \phi(\underline{\omega}))\ ]$$

$$= \frac{1}{2} \int_{R^n} E[\ C^2(d\underline{\omega})\ ] \qquad\qquad \text{(A.28)}$$

(the expectation $E [\cos^2(\underline{\omega}^T \cdot \underline{t} + \phi(\underline{\omega}))]$ is with respect to $\phi(\underline{\omega})$). From (A.19) and (A.28), we obtain :

$$S(\underline{\omega}) \ d\underline{\omega} \ = \ \frac{1}{2} \ E [\ C^2(d\underline{\omega}) \ ] \tag{A.29}$$

Therefore, we may write $X(\underline{t})$ as :

$$X(\underline{t}) \ = \ \sqrt{2} \int_{R^n} \cos [\underline{\omega}^T \cdot \underline{t} + \phi(\underline{\omega})] \ \sqrt{S(\underline{\omega}) \ d\underline{\omega}} \tag{A.30}$$

where $\phi(\underline{\omega})$ is a random phase angle distributed uniformly and independently between 0 and 2π. We can verify that the random field $X(\underline{t})$ expressed by equation (A.30) has the assumed properties, i.e. $X(\underline{t})$ has zero mean and covariance function $B(\underline{\tau})$, using the following two equations :

$$E [\cos (\underline{\omega}^T \cdot \underline{t} + \phi(\underline{\omega}))] \ = \ 0 \tag{A.31}$$

$$E[\cos (\underline{\omega}_1^T \cdot \underline{t}_1 + \phi(\underline{\omega}_1)) \cos (\underline{\omega}_2^T \cdot \underline{t}_2 + \phi(\underline{\omega}_2))]$$

$$= \begin{cases} 0 & \text{if } \underline{\omega}_1 \neq \underline{\omega}_2 \\ 1/2 \ \cos \underline{\omega}^T \cdot (\underline{t}_1 - \underline{t}_2) & \text{if } \underline{\omega}_1 = \underline{\omega}_2 = \underline{\omega} \end{cases} \tag{A.32}$$

Thus,

$$E[X(\underline{t})] \ = \ 0 \tag{A.33}$$

and

$$E[\ X(\underline{t}_2) \ X(\underline{t}_1) \ ] \tag{A.34}$$

$$= \ 2 \int_{R^n} \int_{R^n} E[\cos(\underline{\omega}_1^T \cdot \underline{t}_1 + \phi(\underline{\omega}_1))\cos(\underline{\omega}_2^T \cdot \underline{t}_2 + \phi(\underline{\omega}_2))] \sqrt{S(\underline{\omega}_1)d\underline{\omega}_1 S(\underline{\omega}_2)d\underline{\omega}_2}$$

$$= \int_{R^n} \cos(\underline{\omega}^T \cdot (\underline{t}_2 - \underline{t}_1)) \ S(\underline{\omega}) \ d\underline{\omega} \ = \ B(\underline{t}_2 - \underline{t}_1)$$

We now consider a practical scheme of the numerical simulation based on the above theoretical background. For the convenience of numerical simulation, it is assumed that the spectral density function $S(\underline{\omega})$ has negligible magnitude outside the rectangle defined by:

$$-\Omega_i \leq \omega_i \leq \Omega_i \qquad (A.35)$$

and we denote a discrete interval in the i-th frequency direction by:

$$\Delta\omega_i = \frac{2\Omega_i}{N_i}, \qquad i = 1, \cdots, n. \qquad (A.36)$$

Then, we obtain the following approximation $\hat{X}(\underline{t})$ of $X(\underline{t})$ from equation (A.30):

$$\hat{X}(\underline{t}) = \sqrt{2} \sum_{k_1=1}^{N_1} \cdots \sum_{k_n=1}^{N_n} \left[S(\omega_{1k_1}, \cdots, \omega_{nk_n}) \, \Delta\omega_1 \cdots \Delta\omega_n \right]^{1/2} \cos(\omega_{1k_1}t_1 + \cdots + \omega_{nk_n}t_n + \phi_{k_1, \cdots, k_n})$$

$$(A.37)$$

where the phase angles $\phi_{k_1, \cdots, k_n}$ are independent and uniformly distributed between 0 and 2π, and

$$\omega_{ik_i} = -\Omega_i + (k_i - \tfrac{1}{2})\,\Delta\omega_i, \qquad k_i = 1, \cdots, N_i, \qquad i = 1, \cdots, n. \qquad (A.38)$$

As defined above, $\hat{X}(\underline{t})$ is a homogeneous periodic random field with period $T_i = \pi / \Delta\omega_i$ in the i-th direction. Equation (A.37) can be used directly for simulating $X(\underline{t})$ by generating a series of random angles $\phi_{k_1, \cdots, k_n}$. The random fields generated by this equation are ergotic, and have zero mean. Also, they have covariance function

$$B(\underline{\tau}) = \sum_{k_1=1}^{N_1} \cdots \sum_{k_n=1}^{N_n} \left[S(\omega_{1k_1}, \cdots, \omega_{nk_n}) \, \Delta\omega_1 \cdots \Delta\omega_n \right] \cos(\omega_{1k_1}\tau_1 + \cdots + \omega_{nk_n}\tau_n)$$

$$(A.39)$$

The generated random field $\hat{X}(t)$ has the same structure as the field $X(t)$ when $\Omega_i \to \infty$, $\Delta\omega_i \to 0$, $i = 1, \cdots, n$.

For one-dimensional and two-dimensional random fields, equation (A.30) becomes :

- one-dimensional fields

$$X(t) = \sqrt{2} \int_{-\infty}^{+\infty} \cos(\omega t + \phi)\sqrt{S(\omega)d\omega} \qquad (A.40)$$

- two-dimensional fields

$$X(t_1,t_2) = \sqrt{2} \int_{-\infty}^{+\infty} \int_{-\infty}^{+\infty} \cos[\omega_1 t_1 + \omega_2 t_2 + \phi(\omega_1,\omega_2)]\sqrt{S(\omega_1,\omega_2)d\omega_1 d\omega_2}$$
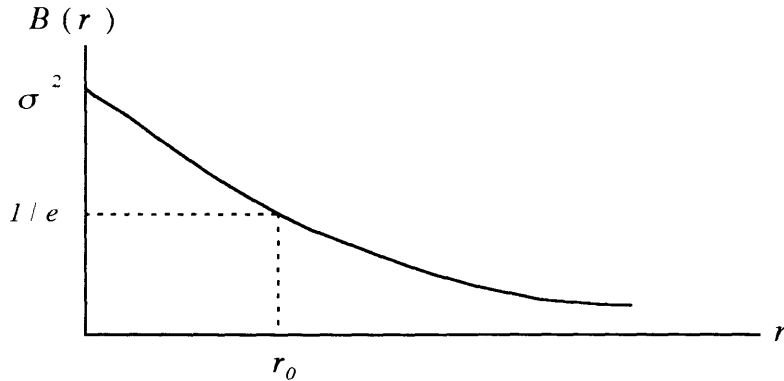
$$(A.41)$$

and equation (A.37) becomes :

- one-dimensional fields
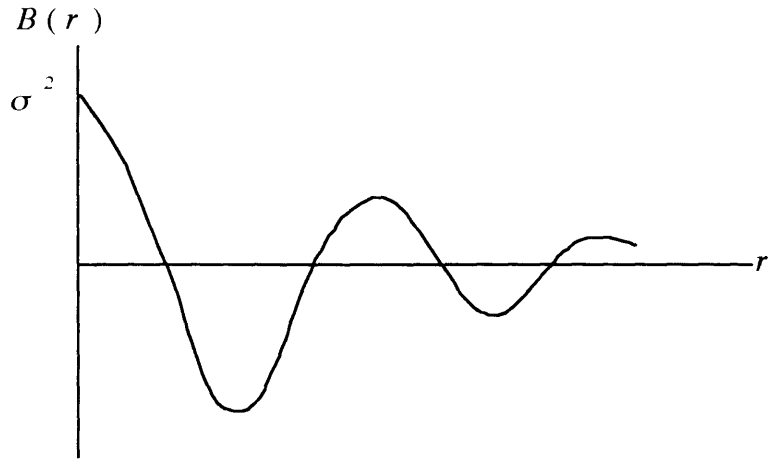
$$\hat{X}(t) = \sqrt{2} \sum_{k=1}^{N} \sqrt{S(\omega_k)\Delta\omega_k} \cos[\omega_k t + \phi] \qquad (A.42)$$

- two-dimensional fields
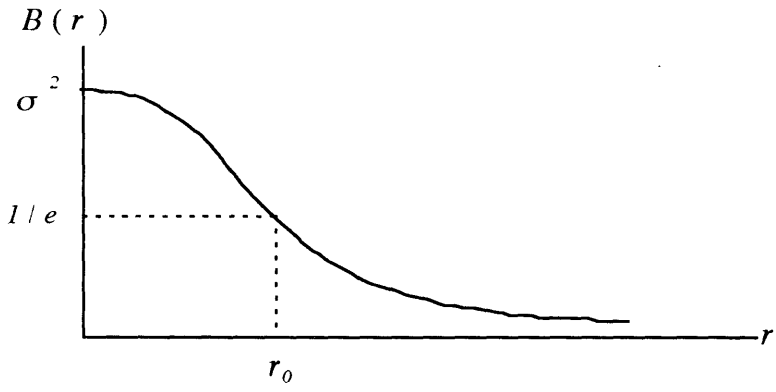
$$\dot{X}(t_1,t_2)$$

$$= \sqrt{2} \sum_{k_1=1}^{N_1} \sum_{k_2=1}^{N_2} \sqrt{S(\omega_{1k_1},\omega_{2k_2})\Delta\omega_1\Delta\omega_2} \cos[\omega_{1k_1}t_1 + \omega_{2k_2}t_2 + \phi_{k_1,k_2}] \quad (A.43)$$
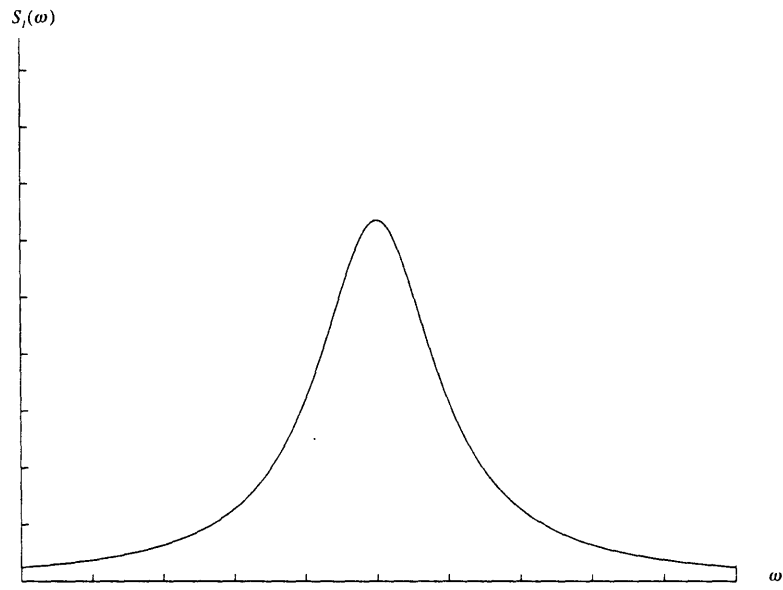
(a) Simple exponential

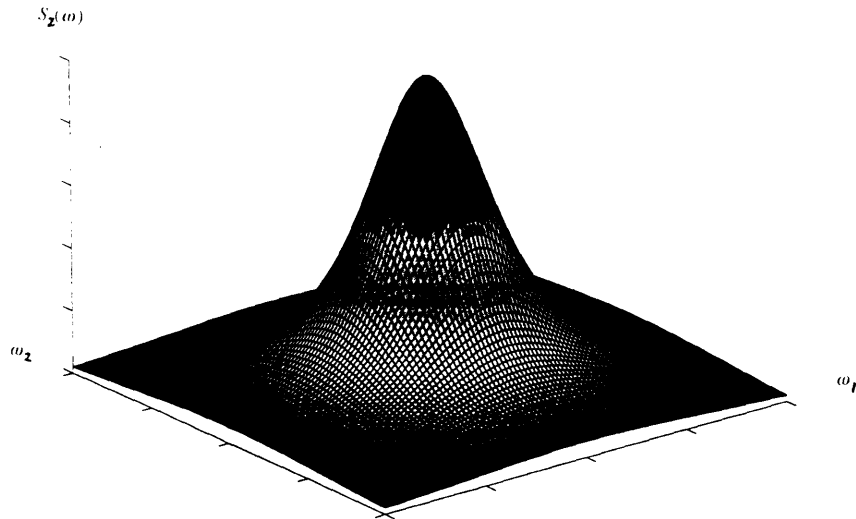(b) Exponentially damped cosine function

(c) Double exponential

Figure A.1 Autocovariance Functions for Isotropic Fields

(a) $S_1(\omega)$

(b) $S_2(\omega)$

Figure A.2 Spectral Density Functions

BIBLIOGRAPHY

Abe, H. (1992) "Two Dimensional Liquefaction Analysis for Ground with Embankment," *Proceedings of the Tenth World Conference on Earthquake Engineering*, Vol. 3, pp.1361~1366, Madrid, Spain.

Bartlett, M. S. and J. E. Besag (1969) "Correlation Properties of Some Nearest-Neighbor Models," *Bull. International Statistical Institute*, Vol. 43, Book 2, pp. 191~193.

Canou, J., A. Bahloul, A. Attar and L. Piffer (1992) "Evaluation of a Liquefaction Criterion for a Loose Sand," *Proceedings of the Tenth World Conference on Earthquake Engineering*, Vol. 3, pp.1367~1372, Madrid, Spain.

Chameau, J. L. and G. W. Clough (1983) "Probabilistic Pore Pressure Analysis for Seismic Loading," *Journal of Geotechnical Engineering Division, ASCE*, Vol. 109, No. 4, pp.507~524.

Christian, J. T. and W. F. Swiger (1975) "Statistics of Liquefaction and SPT Results," *Journal of the Geotechnical Engineering Division, ASCE*, Vol. 101, No. GT33, pp.1135~1150.

Committee on Earthquake Engineering (1985) *Liquefaction of Soils during Earthquakes*, National Academy Press, Washington, D.C.

Davis, R. O. and J. B. Berrill (1981) "Assessment of Liquefaction Potential Based on Seismic Energy Dissipation," *Proceedings of the International Conference on Recent Advances in Geotechnical Earthquake Engineering and Soil Dynamics*, Vol. 1, pp.187~190, University of Missouri, Rolla, Missouri.

Fardis, M. N. (1979) "Probabilistic Liquefaction of Sands during Earthquake," PhD Thesis, Massachusetts Institute of Technology, Department of Civil Engineering.

Fardis, M. N. and D. Veneziano (1982) "Probabilistic Analysis of Deposit Liquefaction," *Journal of the Geotechnical Engineering Division, ASCE*, Vol. 108, No. GT3, pp.395~417.

Halder, A. and W. H. Tang (1979) "Probabilistic Evaluation of Liquefaction Evaluation," *Journal of the Geotechnical Engineering Division, ASCE* , Vol. 105, No. GT2, pp.145~163.

Honjo, Y. (1985) "Dam Filters : Physical Behavior, Probability of Malfunctioning and Design Criteria," PhD Thesis, Massachusetts Institute of Technology, Department of Civil Engineering.

Igarashi, S. (1992) "Energy-Based Factor of Safety Against Liquefaction," *Journal of the Structural Engineering and Earthquake Engineering Division*, Vol. 9, No. 3, pp.181~191, Japan Society of Civil Engineers, Tokyo, Japan.

Iwasaki, T., F. Tatsuoka, K. Tokida and S. Yasuda (1978) "Simple Procedure for Evaluating Liquefaction Potential," *Proceedings of Fifth Japanese Earthquake Engineering Symposium*, pp.641~648 , Tokyo, Japan.

Iwasaki, T., F. Tatsuoka, K. Tokida and S. Yasuda (1980) "Evaluation of Soil Liquefaction Severity," *Soils and Foundations*, Vol. 28, No. 4, pp.23~29, Japanese Society of Soil Mechanics and Foundation Engineering, Tokyo, Japan.

Kafritsas, J. C. (1980) "Some application of Random Field Theory in Geotechnical Engineering," Master's Thesis, Massachusetts Institute of Technology, Department of Civil Engineering.

Kagawa, T. (1988) "Use of Shear-Strain Energy for Liquefaction," *Proceedings of the Ninth World Conference on Earthquake Engineering*, Vol. 3, pp.297~302, Tokyo, Japan.

Kishimoto, S., M. Shinozuka (1989) "Development of Fragility Curves for Liquefaction," *Proceedings of Fifth International Conference on Structural Safety and Reliability*, pp.533~540, ICOSSAR.

Kuwano, J., K. Ozaki and S. Nakamura (1992) "Simplified Method of Liquefaction Hazard Evaluation for Subsurface Layers," *Proceedings of the Tenth World Conference on Earthquake Engineering*, Vol. 3, pp.1431~1434, Madrid, Spain.

Liao, S. S. (1986) "Statistical Modeling of Earthquake-induced Liquefaction," PhD Thesis, Massachusetts Institute of Technology, Department of Civil Engineering.

Oka, F. and Y. Ohno (1988) "Cyclic Plasticity Models for Sand and Clay," *Proceedings of the Ninth World Conference on Earthquake Engineering*, Vol. 3, pp.273~278, Tokyo, Japan.

Prevost, J. H. (1981) "DYNAFLOW : A Nonlinear Transient Finite Element Analysis Program," Department of Civil Engineering, Princeton University, New Jersey.

Prevost, J. H., R. Popescu, K. Hayashi, N. Ohbo and K. Ueno (1992) "Numerical Simulations of Sandy Soil Deposit Liquefaction during Earthquakes," *Proceedings of the Tenth World Conference on Earthquake Engineering*, Vol. 3, pp.1373~1378, Madrid, Spain.

Roach, S. A. (1968) *The Theory of Random Clumping*, Methuen & Co. LTD.

Seed, H. B., and I. M. Idriss (1971) "Simplified Procedure for Evaluating Soil Liquefaction Potential," *Journal of the Soil Mechanics and Foundations Division, ASCE*, Vol. 97, No. SM 9, pp.1249~1273.

Seed, H. B., and I. M. Idriss (1982) *Ground Motions and Soil Liquefaction during Earthquakes*, monograph series, Earthquake Engineering Research Institute, Berkeley, California.

Seed, H. B., K. Tokimatsu, L. F. Harder and R. M. Chung (1985) "Influence of SPT Procedures in Soil Liquefaction Resistance Evaluation," *Journal of the Geotechnical Engineering Division, ASCE* Vol. 111, No. GT12, pp.1425~1445.

Spinkula, D. R. (1983) "Statistical Estimation of Soil Properties and An application," Master's Thesis, Massachusetts Institute of Technology, Department of Civil Engineering.

Stoke, K. H., J. M. Roesset, J. G. Bierschwale and M. Aouad (1988) "Liquefaction Potential of Sands from Shear Wave Velocity," *Proceedings of the Ninth World Conference on Earthquake Engineering*, Vol. 3, pp.213~218, Tokyo, Japan.

Takaya, T., T. Imasato, H. Fukuda and A. Nakazato (1991) "A Way of Making a Microzonation Map of Liquefaction Potential Using the Surface Wave Exploration Method," *Soils and Foundations*, Vol. 39, No. 2, pp.2~34, Japanese Society of Soil Mechanics and Foundation Engineering, Tokyo, Japan, (in Japanese).

Talganov, K. V. (1992) "Application of Strain Approach for Investigation of Post-Initial Liquefaction Behavior of Soils," *Proceedings of the Tenth World Conference on Earthquake Engineering*, Vol. 3, pp.1389~1394, Madrid, Spain.

Tanisawa, F., K. Iwasaki, S. Zhou and F. Tatsuoka (1988) "Evaluation of Liquefaction Length of Sand by Using Cone Penetration Test," *Proceedings of the Ninth World Conference on Earthquake Engineering*, Vol. 3, pp.201~206, Tokyo, Japan.

Tokimatsu, K. and Y. Yoshimi (1983) "Empirical Correction of Soil Liquefaction Based on SPT N-value and Fines Content," *Soils and Foundations*, Vol. 23, No. 4, pp.56~74, Japanese Society of Soil Mechanics and Foundation Engineering, Tokyo, Japan.

Vanmarcke, E (1983) *Random Fields :Analysis and Synthesis*, The MIT Press, Cambridge, Massachusetts.

Veneziano, D. (1978) *Course Notes on Random Processes for Engineering Applications*, Massachusetts Institute if Technology, Cambridge, Massachusetts.

Yaglom, A. M. (1962) *Theory of Stationary Random Functions*, Prentice-Hall, Inc., Englewood Cliffs, New Jersey.

Yegian, M. K., and R. V. Whitman (1978) "Risk analysis for ground failure by liquefaction," *Journal of the Geotechnical Engineering Division, ASCE*, Vol. 104, No. GT7, pp.921~938.

Yasuda, S. (1981) *Liquefaction from Survey to measures*, Kajima Publications, Tokyo, Japan, (in Japanese).